



HAL
open science

The design of resilient food supply chain networks prone to epidemic disruptions

S. M. Gholami-Zanjani, W. Klibi, M. S. Jabalameli, M. S. Pishvae

► To cite this version:

S. M. Gholami-Zanjani, W. Klibi, M. S. Jabalameli, M. S. Pishvae. The design of resilient food supply chain networks prone to epidemic disruptions: .. International Journal of Production Economics, 2021. hal-03422406

HAL Id: hal-03422406

<https://hal.science/hal-03422406>

Submitted on 16 Dec 2022

HAL is a multi-disciplinary open access archive for the deposit and dissemination of scientific research documents, whether they are published or not. The documents may come from teaching and research institutions in France or abroad, or from public or private research centers.

L'archive ouverte pluridisciplinaire **HAL**, est destinée au dépôt et à la diffusion de documents scientifiques de niveau recherche, publiés ou non, émanant des établissements d'enseignement et de recherche français ou étrangers, des laboratoires publics ou privés.

The design of resilient food supply chain networks prone to epidemic disruptions

Seyed Mohammad Gholami-Zanjani ^{a,b}, Walid Klibi ^b, Mohammad Saeed Jabalameli ^a, Mir Saman Pishvaei ^a

^a School of Industrial Engineering, Iran University of Science and Technology, Tehran, Iran

^b The Centre of Excellence in Supply Chain (CESIT), KEDGE Business School, France

se_gholami@ind.iust.ac.ir (S.M. Gholami-Zanjani)

jabal@iust.ac.ir (M.S. Jabalameli)

walid.klibi@kedgbs.com (W. Klibi)

pishvaei@iust.ac.ir (M.S. Pishvaei)

The design of resilient food supply chain networks prone to epidemic disruptions

Abstract

Food supply chains are nowadays perturbed by an increased supply and demand uncertainty, and more and more suffering from unexpected disruptions. In the specific context of food supply chains (FSC) for perishable products, these could be linked to natural hazards, industrial accidents or epidemics and their impact could lead to huge economic losses. The case of epidemic events has been little studied in the existing literature, although there are numerous cases reported in practice. At the strategic level, this requires a novel risk modeling approach to tackle the correlation and propagation features and advanced stochastic multi-period models to design the FSC network. Our interest in this research is to propose a comprehensive two-stage scenario-based mathematical model to design a resilient food supply chain under demand uncertainty and epidemic disruptions. In order to adequately characterize epidemic disruptions, they are modeled as a compound stochastic process and a Monte Carlo procedure is developed to generate plausible scenarios. The modeling approach covers the special characteristics of FSC, such as products perishability in time and discount prices based on product's age. In addition, a number of resiliency strategies are incorporated into the core model to enhance the resilience level of the FSC network design. The developed models are solved through an efficient solution approach relying on scenario reduction technique and Benders decomposition. Numerous problem instances are used to validate the modeling approach and to derive managerial insights.

Keywords: Food Supply Chain, Resiliency, Epidemic Disruptions, Uncertain Demands, Stochastic Programming

1. Introduction

There is no aspect of everyday life more critical than the means by which the world is fed ([Bourlakis & Weightman 2004](#)). The food supply chain (FSC) is considered to be one of the main infrastructures as its continuous flow provides welfare and security for customers and profit for companies involved. The optimization of FSCs was extensively studied in the last decade from efficiency ([Mohan et al., 2013](#)), sustainability ([Validi et al, 2014](#)), quality ([Rong et al, 2011](#)), and robustness ([Vlajic et al, 2012](#)) facets. At the strategic level, the design of FSCs involves the location of a set of capacitated production and distribution facilities and the determination of their mission in order to serve efficiently and durably a customer base. When food products are considered, the problem complexity is usually raised because it deals additionally with limited shelf-life of products, safety requirements, pricing issues and an increased concern for resiliency ([Dani & Deep, 2010](#); [Behzadi et al., 2017](#)). Here, perishability of products imposes a geographical and temporal traceability of the product flow and age along the SC. In addition, the price of a product is dependent on product age in order to control demand and increase revenue ([Goh, 1992](#); [Goh & Sharafali, 2002](#); [Wang & Li, 2012](#); [Kaya & Polat, 2017](#); [Grillo et al., 2017](#)). Moreover, from an inventory management perspective, the inventory holding cost also is linked to the effort required to keep the inventory safe

and to preserve its freshness (San-José et al, 2015). A typical example is meat or poultry supply chain where preservation methods along time are critical. All these elements make the design of FSCs a worthy to study context but a challenging optimization problem, especially under uncertainty.

Moreover, it is well established that SCs evolve in an uncertain environment prone to business-as-usual and to disruptive events (Ponomarov; 2012, Klibi et al.; 2010, Tang; 2006). FSCs are subject to business-as-usual uncertainty typically related to market demand and costs caused by internal and external factors (Behzadi et al., 2018, Vlajic et al., 2012). Additionally, FSCs are increasingly exposed to multiple derivers of disruptions posed by various type of uncertainties such as natural disasters, extreme weather, economic and political crisis, industrial accidents, and so on (Tendall et al. 2015, Stone & Rahimifard, 2018). Further, in the food context, biological deliberate acts and epidemic outbreaks could be additional sources of unavoidable SC disruptions (Manning et al. 2005, Tendall et al. 2015, Gonzalez, 2011, Torabi et al., 2016). According to the World Economic Forum (WEF) risk report in 2019, the world has entered a new era of epidemic risk (Brende, 2019). This report underlined that past outbreaks indicate important contributions from the areas of supply chain and logistics in an effective epidemic readiness. However, a lack of anticipation was observed as we are still moved by the dramatic descriptions from the past (Schwab & Brende, 2018). The COVID-19 crisis shown the vulnerability of agro-food products because it provoked farmers' and workers' illness and thus critical losses in productivity and in production of food products in the USA (<https://ag.purdue.edu/agecon/Pages/FoodandAgVulnerabilityIndex.aspx>). A well-known example of a food epidemic disruption is the Salmonella outbreak through peanut butter in the USA (Terrerri, 2009). Another noticeable example is Avian Influenza crisis that affected the whole poultry chain in several countries and incurred losses of about 200 million Euros to the French poultry industry in 2006 (Le Hoa Vo & Thiel, 2011). Epidemic outbreaks may occur in the context of natural causes, such as the outbreak of novel influenza A (H1N1) virus (WHO, 2010) or linked to a deliberated act such as smallpox and anthrax that are considered as biological agents (Henderson, 1999). When inspecting closely all these cases, it is clear that such disruptions are unexpected and highly impacting events for the FSC which argue for the necessity to anticipate, at the design level, their impact on the business continuity. It is also noticeable that epidemic events are characterized by a specific SC disruption profile and propagation behavior (Dasaklis et al., 2012), and thus the consideration of the spread of disruptions on the FSC network facilities and inventories is crucial. Although their increasing threat, only few studies modeled the risk of epidemic disruptions and investigated its impact on FSCs.

Furthermore, to cope with disruptions in SCs, the field of resiliency has aroused interest worldwide in the last decade. The resiliency concept enhances the ability of SCs to quickly return to their normal performance level after disruption (Sheffi, 2007). Examples of resilience strategies include multiple-sourcing, capacity expansion, product substitution, backup facilities and so on (Tang 2006, Klibi and Martel 2012a). Tendall et al. (2015) defined food system resilience as “the capacity over time of a food system and its units at multiple levels, to provide sufficient, appropriate and accessible food to all, in the face of various and even unforeseen disturbances”. Resiliency strategies could be reactive or proactive: proactive strategies are applied before disruption occurrence, like preservation methods, staff training, vaccination, positioning and strengthening, etc., while reactive strategies are applied in the aftermath of disruptions. Recent reviews of supply chain resilience approaches are found in Kamalahmadi & Parast, (2016) and in Tukamuhabwa et al., (2015). In fact, when a food epidemic disruption occurs, a series of actions are often taken that include stopping the propagation and identifying its source and cause (Terrerri, 2009). These result in shutting down infected or suspicious facilities in the supply chain network. For instance, the author reported that during the Salmonella outbreak in the USA, one of the main reasons for the buoyancy was the continued production of peanut products. Accordingly, the design of FSCs prone to epidemic disruptions necessitates the inclusion of modeling constructs enhancing the resilience of the SC network design, through advanced stochastic multi-period modeling and epidemic risk modeling approaches. Despite the growing efforts to design resilient SC networks, more work needs to be done to quantify resilience (Klibi et al. 2018) and to model resilience-seeking strategies (Ivanov et al. 2019). To the best of our knowledge, no specific epidemic risk modeling approach was developed in the FSC context and applied in a stochastic setting to design resilient SC networks.

With this in mind, the aim of this paper is to propose a comprehensive modeling approach to design a resilient food supply chain network prone to epidemics. The modeling approach presents a multi-period setting to cover the special characteristics of FSCs, such as products perishability and product’s age-based discount prices. It also proposes a novel scenario-based approach in order to model the stochastic processes characterizing the arrival and the impact of epidemic disruptions on the FSC network, as well as the risk of propagation. To cope with such uncertainties, we incorporate a number of resiliency strategies into the core model to enhance the resilience level of the SC network. All these features lead to a two-stage multi-period stochastic program with a challenging solvability. To this end, an efficient solution approach combining a Monte-Carlo procedure, a scenario reduction

method and accelerated Benders decomposition, is proposed to solve a bench of problem instances. The rest of this article proceeds as follows. [Section 2](#) is dedicated to a literature review. [Section 3](#) presents the model development including the problem description, notations and model formulation and the epidemic risk modeling approach. [Section 4](#) presents the modeling approach to integrate the resiliency strategies into the core model. The solution approach is provided in [Section 5](#). [Section 6](#) presents the model validation, numerical results and managerial insights. [Section 7](#) presents some concluding remarks.

2. Literature Review

This section presents key related work in the relevant areas of resilient SC network design and FSCs optimization under uncertainty. In a generic way, several papers attempted to cover the supply chain network design (SCND) problem under disruptions. A critical review of SCND problems under uncertainty is provided in [Klibi et al. \(2010\)](#) where major disruptions provoking SC network deficiencies are listed, and the resilience strategies to consider at the design level are discussed. [Goh et al. \(2007\)](#) investigated supply, demand and disruption risk in a multi-stage global SCND dealing with location and distribution decisions. [Qi et al. \(2010\)](#) investigated SCND with supply disruptions with a model providing location of facilities and allocation of customers to retailers. [Klibi & Martel \(2012a\)](#) proposed different distribution strategies to design a resilient SCND and integrated them into a stochastic multi-period setting.

The concept of network resilience has important implications in understanding supply chain network disruptions ([Sheffi, 2007](#)) and the current literature trend confirms the growing interest by academics and practitioners ([Wagner & Neshat, 2010](#); [Chopra & Sodhi, 2004](#)). Resiliency strategies aim to mitigate disruptions threatening continuity of operations in SCs. These strategies could be categorized as proactive or reactive and from another perspective they could be flexibility, robustness or redundancy strategies ([Faturechi & Miller-Hooks, 2014](#)). [Sawik \(2013, 2014\)](#) applied redundancy and flexibility by keeping safety stock. However, these studies merely focus on the resiliency strategies and do not deeply investigate types of disruptions and their behavior. Some of the recent research in the related literature is summarized in [Table 1](#). Basically, there are two inclusion criteria considered in selecting the papers to be reviewed in [Table 1](#). First, papers that have studied resilient SCND with mathematical models and second, papers that have considered food SC network design models. One should notice that other research streams related to SC reliability ([Du et al., 2020](#)) and to ripple effect ([Ivanov et al., 2014](#), [Ivanov et al., 2019](#)) in the SC,

covered to some extent the notions of resilience and disruptions using alternative modeling approaches. This table shows that most of the studies present generic modeling approaches (i.e. not industry/sector specific), which in the case of the food supply chain is limiting because it doesn't necessarily include critical functional expansions related to limited shelf-life of products, safety requirements, pricing issues and resiliency to epidemics.

From another perspective, disruptions can be divided into two categories: single and multiple. By single disruption, when a facility is affected, it can recover after a certain period, while in multiple disruptions an affected facility may be disrupted again before full recovery. To the best of our knowledge and according to Table 1, most studies have only discussed single disruptions and only a few studies consider multiple disruptions. By single disruptions, generally, a facility is disrupted fully or partially just once in the planning horizon considered. Klibi & Martel (2012b) studied multiple disruptions occurring in time and space. They assumed that natural disasters, and industrial accidents could happen at the facilities according to their vulnerability and risk exposure level. Unlike single disruption setting, these disruptions could happen concurrently at the same facilities of the network and more than once during the planning horizon. Moreover, correlated disruptions are special cases in multiple disruptions category that no research has been conducted on it as the epidemic disruptions. It is clear that disruptions are multi-phase and their modeling makes sense through a multi-period setting. However, as highlighted in Table 1, only few studies have implemented disruption behavior through a multi-period time horizon. Finally, it is worth mentioning that disruption occurrence may affect different SC network resources and regarding Table 1, most studies have assumed that it will affect the facility capacity, while inventory drop out has been neglected so far.

Table 1 A summary of resilient supply chain network design literature

Authors	Year	Multi-period	network stages	perishability	Uncertainty type				Modeling Framework	Solution method		Resiliency strategies	Application area
					Business-as-usual	Disruption effect		Disruption type		Exact	Heuristic		
						Inventory	Capacity						
Amiri-Aref et al.	2018	•	3	-	•	-	-	-	SP	-	-	Ms	general
An & Ouyang	2016	-	3	-	•	-	-	-	RO	-	-	-	grain
Azad et al.	2012	-	2	-	-	-	•	S	-	•	-	-	general
Baghalian et al.	2013	-	3	-	•	-	•	S	SP	-	-	-	general
Fahimnia & Jabbarzadeh	2016	-	3	-	•	-	•	S	SP	-	-	-	general
Fattahi et al.	2017	•	1	-	•	-	•	S	RO	-	-	F, B	general
Hassani & Khosrojerdi	2016	•	3	-	•	-	•	S	RO	-	•	F,B,D,A	general
Ivanov et al.	2016	•	3	-	-	-	•	S	-	-	-	B,F,C,P	general
Jabbarzadehet al.	2016	-	2	-	•	-	•	S	RO	•	-	F	general
Kamalahmadi & Mellatparast	2015	-	2	-	-	-	•	S	SP	-	-	C	general
Keizer et al.	2017	-	2	•	•	-	-	-	-	-	-	-	general
Klibi & Martel	2012	•	2	-	•	-	•	S, M	SP	-	-	B,Ms,Co	general
Mohammed & Wang	2017	-	3	-	•	-	-	-	FO	-	-	-	meat
Nooraei &	2016	•	5	-	-	-	-	S	SP	-	•	B	general

Mellatparast													
Qin et al.	2013	-	2	-	-	-	•	S	SP	•	-	F,P	general
Rong et al.	2011	•	3	•	-	-	-	-	-	-	-	-	food
Sawik	2018	•	2	-	•	-	•	S	SP	•	-	B	general
Shishebori & Babadi	2015	-	3	-	•	-	•	S	SP	-	-	-	general
Soysal et al.	2014	-	4	-	-	-	-	-	-	-	-	-	beef
Validi et al.	2014	•	2	•	-	-	-	-	-	-	•	-	dairy
Zahiri et al.	2017	•	4	-	•	-	-	-	FO	-	•	B, N	pharmaceutical
Zahiri et al.	2018	•	3	•	•	-	-	-	FO	-	-	-	pharmaceutical
<i>This research</i>		•	3	•	•	•	•	S, M	SP	•	-	F,B,C,Ms	food
S: single disruption M: multiple disruptions		SP: stochastic programming RO: robust optimization FO: fuzzy optimization			F: fortification D: facility dispersion B: backup suppliers			P: prepositioning Co: coverage formulation C: capacity expansions			N: network complexity A: alternative BOM Ms: multiple assignment		

The other stream of literature relevant to this study is FSCs under uncertainty. Much progress has been made in the field of food supply chain management (Mohan et al., 2013; Soysal et al., 2015, De Keizer et al., 2017). Rong et al. (2011) incorporated food quality into the multi-period production and distribution planning problem of a two-stage network. They developed a mixed integer linear programming (MILP) model minimizing total costs including production, transportation, inventory and waste disposal along with the cooling cost of transportation equipment and storage facilities. Additionally, Validi et al. (2014) presented a multi-objective model for the design of a capacitated distribution network for a two-echelon Irish dairy market supply chain. Bortolini et al. (2016) developed a linear programming model to deal with the tactical optimization problem of fresh food distribution networks. They were concerned with carbon footprint and delivery time objectives as well as considering producers and retailers along with constraints on food quality, production capacity and market demand. Mohammed & Wang (2017b) developed a three-echelon meat supply chain network design model, which includes number and location of facilities to be established. Besides minimizing associated cost, environmental objective function is also considered through a fuzzy multi-objective approach. Mogale et al. (2018) investigated food grain supply chain network design in India using a multi-period deterministic modeling approach.

Recently, Mohammed & Wang (2017a) and Mohammed et al. (2017) studied meat supply chain network design investing on RFID for tracing the product through the network. Traceability of food products is a very important issue for most food manufacturing companies since potential risks such as contaminations could be propagated. Although extensive research has been conducted in this regard (Dupuy et al., 2005; Rong & Grunow, 2010; Aung & Chang, 2014), it is not integrated in current SC network design frameworks. Vlajic et al. (2012), Estes et al., (2018) and Stone et al. (2018) proposed a conceptual framework to design robust food supply chains, but no modeling approach is proposed. They defined sources of FSCs vulnerability and redesign strategies to achieve robust and resilient SC performance. An & Ouyang (2016) developed a bi-level robust optimization model for profit

maximization and post-harvest loss minimization of a food company by considering farmers, storage facilities and export markets. Regarding the inventory models in this context, there are several researches that have adopted the specific features of food products (Jaggie et al., 2017; Tiwari et al., 2018). However, they did not consider the network design and disruption simultaneously.

Motivated by these studies and numerous cases in practice, this paper bridges a gap in resilient food supply chain network design (RFSCND) with novel SC risk and design modeling approaches. Although some papers have addressed related aspects (Table 1), to the best of our knowledge, none of them has investigated SCND with food products' characteristics, such as perishability, product age-dependent price, and epidemic disruptions. We believe that the integration of these specific characteristics into the design model promote the robustness of the solution produced.

3. Problem context:

In this paper, a food processing and distribution network design problem is studied, inspired from the meat supply chain. The food supply chain network design (FSCND) problem modeled here focuses on finding the optimal configuration of a three-echelon network for perishable products, consisting of processing centers (PCs), distribution centers (DCs)/refrigerated warehouses and retailers, as shown in Figure 1. The proposed model aims to maximize the total expected profit of the company along a multi-period planning horizon. The main decisions addressed by the proposed FSCND model involve the number, location and capacity of PCs and DCs and material flow planning decisions at each facility to open. Locations of PCs and DCs are chosen from a set of candidate sites at the beginning of the planning horizon, since these decisions are strategic.

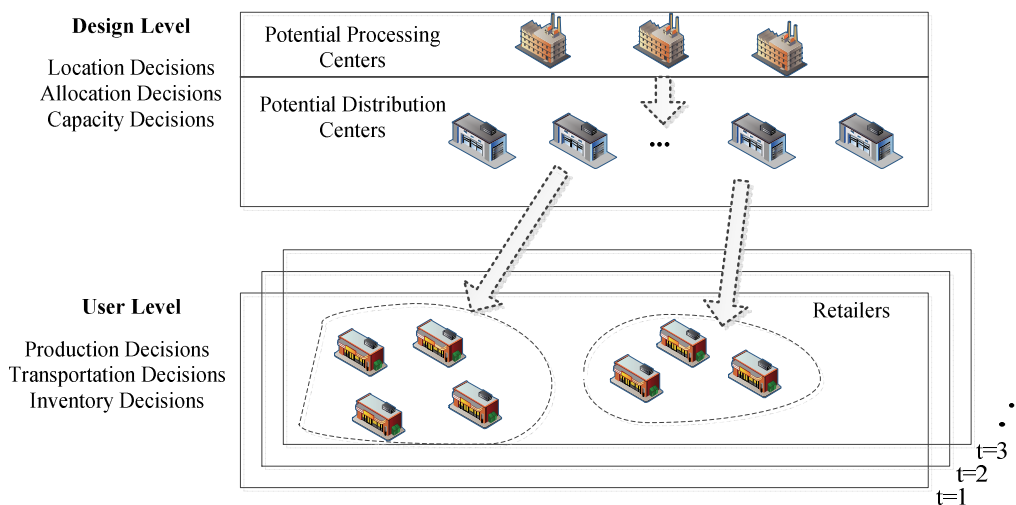


Figure 1 Design and planning levels of the multi-period FSC network

The main characteristics of the food supply chain considered here are described as follows.

- Producing food products involves small to large processing industry facilities. Here, raw materials are collected from farms, crops and other sources, and are transformed, packed, and made ready for storage or distribution. This step could also involve preservation methods such as dehydration and using preservatives. These methods increase the durability of products mainly by removing water and moisture from products or increasing concentration of salt or acids. A set of capacity levels, expressed in throughput, is considered at each potential PC, and only one can be set.
- Distribution of perishable products involves warehousing in refrigerated platforms (i.e. controlled temperature), and then transportation to retailers. These DCs conserve, store and consolidate the products received from the PCs. Refrigerated warehouses preserve the perishable products from decay and postharvest maturation behavior, and monitor their deterioration. At this echelon, we assume that a number of DCs may be established in a set of potential locations and that the throughput capacity level of each DC must be determined.
- Retailers in the FSC are the final actors that deal directly with the consumers, who are widely dispersed in a geographical area. They are replenished by DCs and cannot be replenished directly by the PCs. It is not mandatory to satisfy all demand, and unmet demand is assumed to be lost. A penalty cost for each unit of unsatisfied demand is therefore imposed to the objective function.
- Products considered here have a predetermined remaining shelf life for consumption, as they must be consumed within specific limited period. It is assumed that products produced/processed earlier should be transported to DCs and next to retailers sooner. Hence, the storage system applies a 'first expire, first out' (FEFO) distribution rule. If there are some products in warehouses or with retailers whose remaining shelf life period has expired, they must be disposed of. Here, we suppose that the life time or shelf life of a product begins when it is produced in the PCs. According to the time, temperature, tolerance (TTT) theory presented by [Zwietering et al. \(1996\)](#), the rate of deterioration accelerates as the time period goes on.
- The price of the product is a function of its freshness ([Wang & Li, 2012](#)), which is modeled hereafter using a step-wise price discounting function, as shown in [Figure 2](#). This figure illustrates how the product selling price is estimated according to the age of the product. This latter is measured based on the difference between its processing period and consumption time in order to make the model as general as possible. Since the product

has a predefined shelf life (SL), this means that when the product age becomes more than its SL, the product status is changed to expired. In this case, a practical approach to manage sale revenues is to employ step-wise price discounting similar to the one in Figure 2 where r is the production period of the product and t is the time period in which the product is consumed.

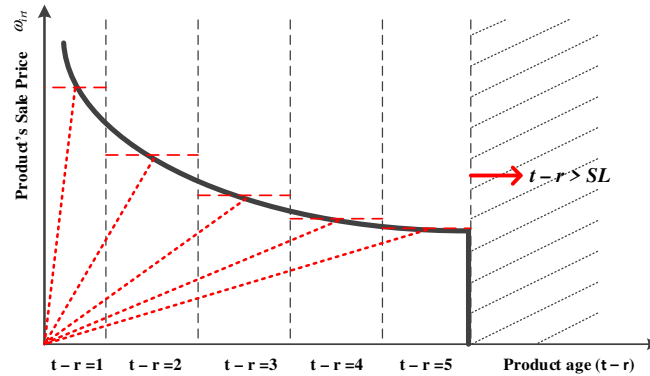


Figure 2 Modeling product sale price versus product age

3.1. Scenario-based FSC design approach

Based on the previous problem definition and considering the following indices, parameters and decision variables, a single-product perishable food production-distribution problem is formulated over the planning horizon as a two-stage programming approach via mixed integer linear programming (MILP). It is assumed that the design horizon is composed of a set of discrete time periods in which weekly or monthly decisions related to product flow are made. The first stage of the model addresses the here and now strategic decisions on the location and capacity level of PCs and DCs among the candidate sites, and assignment decisions between the facilities of the SC network. The second stage of the model corresponds to the tactical planning level where the network material flow, inventory level and demand fulfillment decisions are fixed, once each given scenario is realized. A scenario is the concatenation of a possible sequences of events over the planning horizon. An event is a measurable (i.e. having observable consequences) incident influencing the business environment of the SC network during a given time period. The model's objective function is maximization of expected profit, which is equal to total expected revenue minus total expected cost. Total cost includes facilities' fixed opening cost, production cost, inventory holding cost, transportation cost, lost sales cost and cost of product expiration. The main set of constraints of the proposed model are associated to retailers and DCs assignment, demand satisfaction, production and inventory balance, and capacity levels.

Sets and indices

P	Set of PCs indexed by p ($p \in P$)
D	Set of DCs indexed by d ($d \in D$)
I	Set of retailers indexed by i ($i \in I$)
T	Set of time periods indexed by t & r (t & $r \in T$)
N	Set of possible capacity levels for each PC indexed by n ($n \in N$)
K	Set of possible capacity levels for each DC indexed by k ($k \in K$)
S	Set of plausible scenarios indexed by s ($s \in S$)

Parameters

f_{pn}	Establishment cost of PC p with capacity level n
f_{dk}	Establishment cost of DC d with capacity level k
cap_{pn}	Maximum throughput of PC p at level n for the time period
cap_{dk}	Maximum throughput capacity of DC d at level k for the time period
cap_i	Maximum inventory holding capacity of retailer i for the time period
q_p	Production capacity of PC p for the time period
c_{pd}	Unit transportation cost associated with going from PC p to DC d
c_{di}	Unit transportation cost associated with going from DC d to retailer i
c_p	Unit production cost at PC p
h_p	Unit inventory holding cost for PC p for the time period
h_d	Unit inventory holding cost for DC d for the time period
h_i	Unit inventory holding cost for retailer i for the time period
ls_{it}	Unit lost-sale cost for retailer i at time period t
d_{it}^s	Demand of product in retailer i at time period t , under scenario s
sl	Shelf life of product in time periods
ω_{irt}	Price of product in retailer i in period t for the product which is produced in period r
ce_{pt}	Unit expiration cost of product at PC p at time period t
ce_{dt}	Unit expiration cost of product at DC d at time period t
ce_{it}	Unit expiration cost of product at retailer i at time period t
$P(s)$	Occurrence probability of scenario s
M	A large number

First-stage decision variables

L_{pn}	Equals 1 if a PC is established in potential location p with capacity level n , otherwise 0
L_{dk}	Equals 1 if a DC is established in potential location d with capacity level k , otherwise 0
A_{id}	Equals 1 if retailer i is assigned to DC d , otherwise 0

Second-stage decision variables

y_{irt}^s	Amount of product delivered to customers in retailer i at period t , which is produced in time period r , under scenario s
Pr_{pr}^s	Amount of product produced at time period r in PC p , under scenario s
x_{pdrt}^s	Amount of product produced at period r and transported to DC d from PC p in time period t , under scenario s
x_{dirt}^s	Amount of product produced in period r and transported to retailer i from DC d in time period t , under scenario s
I_{prt}^s	Amount of product produced in period r and remaining until end of period t in PC p , under scenario s

I_{drt}^s	Amount of product produced in period r and remaining until end of period t in DC d , under scenario s
I_{irt}^s	Amount of product produced in period r and remaining until end of period t in retailer i , under scenario s
D_{it}^{-s}	Amount of lost-sale for demand in time period t and retailer i , under scenario s
E_{it}^s	Amount of product expired at time period t and retailer i , under scenario s
E_{pt}^s	Amount of product expired at time period t in PC p , under scenario s
E_{dt}^s	Amount of product expired at time period t in DC d , under scenario s

Mathematical formulation:

The first-stage model optimizes the location, capacity and allocation decisions. Objective function (1) maximizes the second-stage objective function minus total strategic cost, which includes PC and DC establishment costs. Let \mathbf{x} denote the vector of second-stage decision variables and for the given set of scenarios \mathbf{s} , $Q(\mathbf{x}, \mathbf{s})$ is the optimal objective value of the second-stage problem.

$$\text{Max } Z = \sum_{s \in \mathbf{S}} p(s) Q(\mathbf{x}, s) - \sum_{p \in P} \sum_{n \in N} f_{pn} L_{pn} - \sum_{d \in D} \sum_{k \in K} f_{dk} L_{dk} \quad (1)$$

Constraints:

Each PC and DC can be established with only one capacity level stated by Constraints (2) and (3).

$$\sum_n L_{pn} \leq 1 \quad \forall p \in P \quad (2)$$

$$\sum_k L_{dk} \leq 1 \quad \forall d \in D \quad (3)$$

Constraints (4) ensure that retailer i is assigned to DC d only if a DC is opened in location d . Constraints (5) ensure that each retailer should be assigned to a single DC.

$$A_{id} \leq \sum_k L_{dk} \quad \forall i \in I, d \in D \quad (4)$$

$$\sum_{d \in D} A_{id} = 1 \quad \forall i \in I \quad (5)$$

The second-stage objective function (6) maximizes total expected revenue with respect to the set of scenarios.

Second-stage costs include production cost, transportation costs from PCs to DCs and from DCs to retailers, inventory holding cost in PCs, DCs and retailers, lost sales penalty at retailers and product expiration cost at each level of the SC. It is worth mentioning that if the amount of delivered product is predetermined, then the first term is constant and it is sufficient to minimize the cost terms. Otherwise, the amount of product, combination of different ages, becomes a decision variable. Demand is considered to be bounded ($d_{it} \leq d_{it}^s$), where d_{it} is a lower bound as a market share target which could be estimated through the marketing positioning strategy of the company.

$$\begin{aligned}
Q(\mathbf{x}, s) = & \sum_{i \in I} \sum_{r \in T} \sum_{t \in T | r \leq t} \omega_{irt} y_{irt}^s - \\
& \left(\sum_{p \in P} \sum_{t \in T} c_p Pr_{pt}^s + \sum_{p \in P} \sum_{d \in D} \sum_{r \in T} \sum_{t \in T | r \leq t} c_{pd} x_{pdr}^s + \sum_{d \in D} \sum_{i \in I} \sum_{r \in T} \sum_{t \in T | r \leq t} c_{di} x_{dir}^s \right. \\
& + \sum_{p \in P} \sum_{r \in T} \sum_{t \in T | r \leq t} h_p \left(\frac{I_{prt-1}^s + I_{prt}^s}{2} \right) + \sum_{d \in D} \sum_{r \in T} \sum_{t \in T | r \leq t} h_d \left(\frac{I_{drt-1}^s + I_{drt}^s}{2} \right) + \sum_{i \in I} \sum_{r \in T} \sum_{t \in T | r \leq t} h_i \left(\frac{I_{irt-1}^s + I_{irt}^s}{2} \right) \\
& \left. + \sum_{p \in P} \sum_{t \in T} ce_{pt} E_{pt}^s + \sum_{d \in D} \sum_{t \in T} ce_{dt} E_{dt}^s + \sum_{i \in I} \sum_{t \in T} ce_{it} E_{it}^s + \sum_{i \in I} \sum_{t \in T} ls_{it} D_{it}^{-s} \right) \quad (6)
\end{aligned}$$

According to [Constraints \(7\)](#), product can be transported from DC d , to retailer i , if and only if retailer i is assigned to DC d . Similarly, [Constraints \(8\)](#) set transportation requirement from a given center p to a DC d .

$$x_{dir}^s \leq M \times A_{id} \quad \forall d \in D, i \in I, r \& t \in T \mid 0 \leq t - r \leq SL, s \in S \quad (7)$$

$$x_{pdr}^s \leq M \sum_n L_{pn} \quad \forall p \in P, d \in D, r \& t \in T \mid 0 \leq t - r \leq SL, s \in S \quad (8)$$

[Constraints \(9\)](#), [\(10\)](#) and [\(11\)](#) show the inventory balance in PCs for each time period. In other words, at the end of each time period, the amount of product which is produced in time period r is equal to the amount of product at the end of the previous period minus the sum of the amount sent to the DCs, or it is changed to expired if its age is more than the shelf life.

$$Pr_{pr}^s = I_{pr}^s + \sum_{d \in D} x_{pdr}^s \quad \forall p \in P, r \& t \in T \mid r = t, s \in S \quad (9)$$

$$I_{prt}^s = I_{pr(t-1)}^s - \sum_{d \in D} x_{pdr}^s \quad \forall p \in P, r \& t \in T \mid 0 < t - r \leq SL, s \in S \quad (10)$$

$$\sum_{r \in T \mid t-r=SL} I_{prt}^s = E_{pt}^s \quad \forall p \in P, t \in T, s \in S \quad (11)$$

[Constraints \(12\)](#), [\(13\)](#) and [\(14\)](#) show the inventory balance at DCs for each time period.

$$\sum_{p \in P} x_{pdr}^s = I_{dr}^s + \sum_{i \in I} x_{dir}^s \quad \forall d \in D, r \& t \in T \mid r = t, s \in S \quad (12)$$

$$I_{drt}^s = I_{dr(t-1)}^s + \sum_{p \in P} x_{pdr}^s - \sum_{i \in I} x_{dir}^s \quad \forall d \in D, r \& t \in T \mid 0 < t - r \leq SL, s \in S \quad (13)$$

$$\sum_{r \in T \mid t-r=SL} I_{drt}^s = E_{dt}^s \quad \forall d \in D, t \in T, s \in S \quad (14)$$

[Constraints \(15\)](#) and [\(16\)](#) show the inventory balance at the retailers' echelon for each time period. Here, all orders are assumed to be delivered within less than a time period which equals zero.

$$\sum_{d \in D} x_{dir}^s = I_{it}^s + y_{it}^s \quad \forall i \in I, r \& t \in T \mid r = t, s \in S \quad (15)$$

$$I_{irt}^s = I_{ir(t-1)}^s + \sum_{d \in D} x_{dir}^s - y_{it}^s \quad \forall i \in I, r \& t \in T \mid 0 < t - r \leq SL, s \in S \quad (16)$$

[Constraints \(17\)](#) define the amount of expired products in each time period at the retailer's location.

$$\sum_{r \in T | t-r=SL} I_{it}^s = E_{it}^s \quad \forall i \in I, t \in T, s \in S \quad (17)$$

Constraints (18) and (19) are related to demand satisfaction. Constraints (18) ensure that the minimum demand at each time period for each retailer site is satisfied. Constraints (19) balance demand, lost-sale and products delivered to customers. As it can be seen, the delivered products could be combination of different product ages.

$$\sum_{r \in T | 0 < t-r \leq SL} y_{it}^s \geq \underline{d}_{it} \quad \forall i \in I, t \in T, s \in S \quad (18)$$

$$\sum_{r \in T | 0 < t-r \leq SL} y_{it}^s + D_{it}^{-s} = d_{it}^s \quad \forall i \in I, t \in T, s \in S \quad (19)$$

Constraints (9) – (19) model the requirements of products flow along the SC stages and over the periods. In order to measure product age at each network node and time period, an alias index (r) is introduced to show the time period in which the product is processed, in other words, its base time. This is further depicted in Figure 3 with an example. It illustrates the product flow in the network for periods 1, 2 till t , for the product units that are processed in period ($r=1$). This shows how product units are controlled and get older through the SC based on their processing period. As for the ageing process, in each time period, the difference between the current time period and processing time period ($t - r$) shows product age.

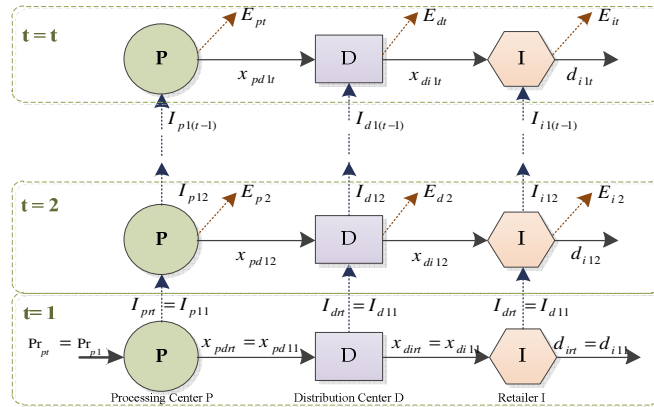


Figure 3 Product flow and ageing process for processed amount in period one ($r = 1$)

Constraints (20) show the production capacity of each PC in each time period.

$$Pr_{pr}^s \leq q_p \quad \forall p \in P, r \in T, s \in S \quad (20)$$

Constraints (21), (22) and (23) represent the throughput capacity of PCs and DCs, and inventory capacity of retailers, respectively. It is clear that these constraints are interconnected with the balance Constraints (9) -(17) and the flows are limited by the capacities.

$$\sum_{d \in D} \sum_{\substack{r \in T \\ 0 \leq r \leq t}} x_{pdr}^s \leq \sum_n cap_{pn} L_{pn} \quad \forall p \in P, t \in T, s \in S \quad (21)$$

$$\sum_{i \in I} \sum_{\substack{r \in T \\ 0 \leq r \leq t}} x_{dir}^s \leq \sum_k cap_{dk} L_{dk} \quad \forall d \in D, t \in T, s \in S \quad (22)$$

$$\sum_{r \in T | 0 \leq r \leq t} I_{int}^s \leq cap_i \quad \forall i \in I, t \in T, s \in S \quad (23)$$

Constraints (24) and (25) are related to types of variables.

$$L_{pn}, L_{dk}, A_{id} \in \{0,1\} \quad \forall p \in P, n \in N, d \in D, k \in K, i \in I \quad (24)$$

$$x_{pdr}^s, x_{dir}^s, Pr_{pr}^s, I_{prt}^s, I_{drt}^s, I_{int}^s, \quad \forall p \in P, d \in D, i \in I, r \in T, t \in T, s \in S \quad (25)$$

$$E_{it}^s, E_{dt}^s, E_{pt}^s, D_{it}^{-s}, y_{int}^s \geq 0$$

3.2. Modeling the Epidemic disruption process

As mentioned, this work investigates the resilience of the FSCND, prone to epidemic disruptions. Such disruptions have a cascading impact and when a facility is hit, other facilities are also under the threat of disruption. Such correlation is due to the geographical proximity and/or to the inter-sites flows. These disruptions are mainly characterized by their intensity, time to recovery of facilities and propagation among facilities. Accordingly, we propose in this section a probabilistic modeling approach for the arrival of epidemic disruptions, their physical impact on FSC resources and their propagation in time on the rest of the SC network. The approach builds on the SC risk modeling framework proposed by [Klibi and Martel \(2012b\)](#) to integrate the main characteristics of epidemic risk and the specific impact on FSCs. It also takes bases on the so-called susceptible-infectious-recovered (SIR) model extensively used for the management of infectious diseases ([Tassier, 2005](#)).

The schematic representation of the arrival of an epidemic disruption in the network is depicted in [Figure 4](#). As illustrated, when an epidemic disruption hits at time t , a primary facility is first attained, but all the network resources in the surrounding region of the hit zone and those in relation with that resource are exposed to propagation risk. So, based on the flow level between each pair of nodes and the distance between them, the propagation of the disruption could spread in the subsequent periods ($t+1, t+2, \dots$) which become themselves contaminated nodes, and so on. To do so, a correlation matrix is used for propagation probabilities in which values are mainly function of regional proximity and of directional network relations. For instance, the disruption propagation is more probable from an upstream PC to downstream DCs assigned to it, than in the opposite direction.

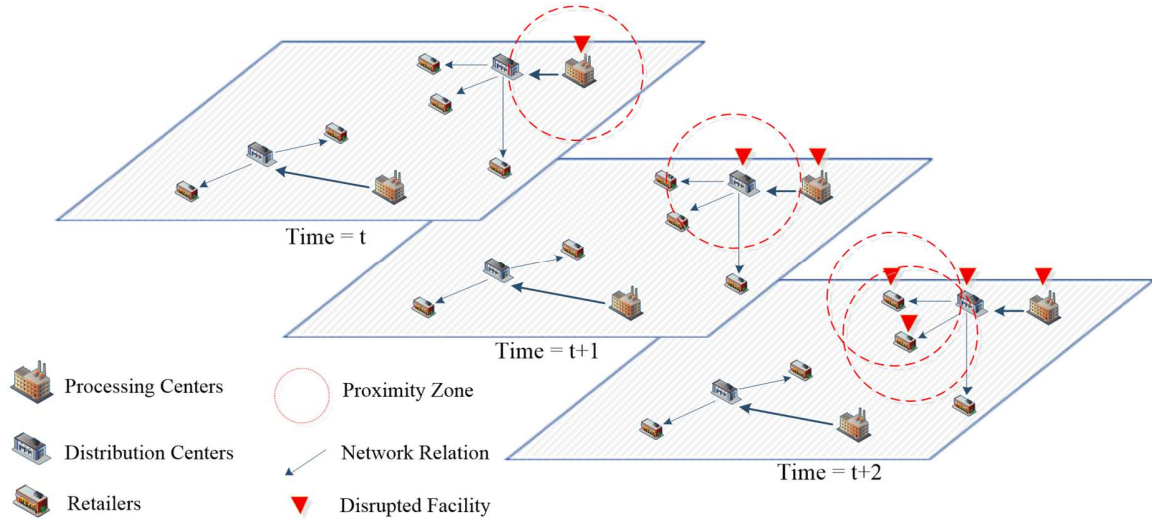


Figure 4 Schematic representation of epidemic disruption in a network

Thus, the proposed modeling approach is based on a stochastic compound process which unveils how events could happen randomly in time over the planning horizon and in space over the geographical region under consideration. It starts with partitioning the region into a set of zones, and defining the exposure level of each zone. So, facilities located in each specific zone inherit of the zone risk exposure level and disruption occurrence characteristics. The next step characterizes disruption attributes including occurrence time and intensity. The final step models impact in terms of recovery duration and in terms of ability of PCs and DCs to ensure operations during the recovery period. In the following, the modeling approach is described in detail, using the notation summarized as follows.

Disruption process notations

Z	Set of zones, partitioning the considered region; $z \in Z$
E	Set of nodes in the network indexed by e ; $e \in E = \{P, D, I\}$
σ_z	Attenuation probability of zone z to be hit by disruptions (zone's risk exposure level)
π_e	Attenuation probability of node e to be hit by disruptions (node's risk exposure level)
β_e^s	Proportion of capacity loss for node e , with values in $[0, 1]$, under scenario s
θ_e^s	Time to recovery for node e in periods, under scenario s
λ_z	Mean time between two consecutive disruptions in zone z
$\alpha_{e z(e)}$	Attenuation probability of node e if its containing zone is hit by a disruption
$c_{e e'}$	Conditional propagation probability of node e when node e' is hit by a disaster

$pro_{e|e'}$ Equals 1 if disruption is propagated from node e' to node e , otherwise 0

For most of the disruption types, when a node is hit by a given event, the severity of the disruption is associated to a given node of the network and is based on two correlated factors, namely, impact intensity and time to recovery. However, in the case of epidemic event, this is not sufficient and thus one must consider the notion of propagation inter-nodes which is another dimension characterizing the severity of a disruption on the FSC network. Next, as well established, disruption does not uniformly affect the network nodes during the recovery time period (Sheffi, 2005) and several phase-dependent impacts can be defined by a discrete and step-wise recovery function (Klibi and Martel, 2012a). In context of food SCs prone to epidemic disruptions, since the suspected facilities are shut down and the suspected inventories are disposed, it is assumed that the throughput capacity and the inventory kept are dropped to zero. The capacity is fully recovered after the time to recovery periods and the inventory level is restored only at the end of the time to recovery based on newly replenished products. Figures 5a) and 5b) mimic, respectively, the impact of an epidemic disruption on the facility capacity and on the inventory level kept within.

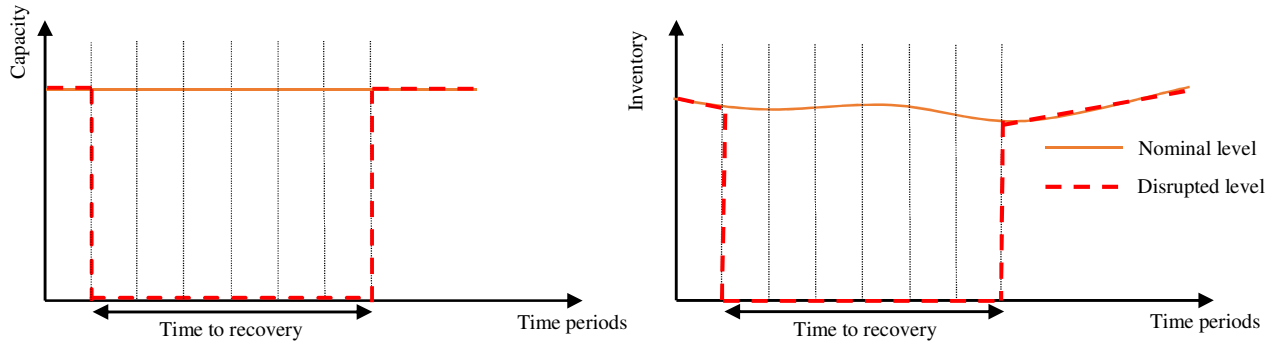


Figure 5 a) Capacity loss-recovery functions

b) Inventory loss-recovery functions

With this modeling approach, the attenuation probability of node e can be computed with Equation (26). It is assumed that node e can be disrupted directly (i.e. is the centroid of a disruption); or it could be disrupted due to the propagation of a disruption hitting other facilities which are in the inter-sites network of node e .

$$\pi_e = \sum_{e' \in E} c_{e|e'} \pi_{e'} + \alpha_{e|z(e)} \sigma_z \quad (26)$$

Regarding Equation (26) and disruption notations, $g_t(\beta_e^s, \theta_e^s)$ is defined as a function to show the impact of disruptions on the capacity and inventory level of network facilities during the disruption time. Its generation process is described in detail in Appendix A. Then, obtained from $g_t(\beta_e^s, \theta_e^s)$, loss parameter ζ_{et}^s is corresponding

to the lost portion of the nominal capacity and inventory level that is generally between 0 and 1 (See Figure 5). This stochastically generated loss parameter is used to reformulate the core mathematical model.

Given the disruption modeling process described above, the design model (1)-(25) must be adapted as follows.

Constraints (21), (22) and (23) are modified, respectively, as follows to take into account capacity disruptions.

$$\sum_{d \in D} \sum_{r \in T} x_{pdr}^s \leq (1 - \zeta_{pt}^s) \left(\sum_n cap_{pn} L_{pn} \right) \quad \forall p \in P, t \in T, s \in S \quad (27)$$

$$\sum_{i \in I} \sum_{r \in T} x_{dir}^s \leq (1 - \zeta_{dt}^s) \left(\sum_k cap_{dk} L_{dk} \right) \quad \forall d \in D, t \in T, s \in S \quad (28)$$

$$\sum_{r \in T} I_{int} \leq (1 - \zeta_{it}^s) cap_i \quad \forall i \in I, t \in T, s \in S \quad (29)$$

With regards to the inventory level, Constraints (9), (10), (12), (13), (15) and (16) become as follows.

$$(1 - \zeta_{pt}^s) Pr_{pt}^s = I_{prt}^s + \sum_{d \in D} x_{pdr}^s \quad \forall p \in P, r \& t \in T \mid r = t, s \in S \quad (30)$$

$$I_{prt}^s = (1 - \zeta_{pt}^s) I_{pr(t-1)}^s - \sum_{d \in D} x_{pdr}^s \quad \forall p \in P, r \& t \in T \mid r < t, s \in S \quad (31)$$

$$(1 - \zeta_{dt}^s) \left(\sum_{p \in P} x_{pdr}^s \right) = I_{drt}^s + \sum_{i \in I} x_{dir}^s \quad \forall d \in D, r \& t \in T \mid r = t, s \in S \quad (32)$$

$$I_{drt}^s = (1 - \zeta_{dt}^s) \left(\sum_{p \in P} x_{pdr}^s + I_{dr(t-1)}^s \right) - \sum_{i \in I} x_{dir}^s \quad \forall d \in D, r \& t \in T \mid r < t, s \in S \quad (33)$$

$$(1 - \zeta_{it}^s) \left(\sum_{d \in D} x_{dir}^s \right) = I_{drt}^s + y_{int}^s \quad \forall i \in I, r \& t \in T \mid r = t, s \in S \quad (34)$$

$$I_{int}^s = (1 - \zeta_{it}^s) \left(I_{ir(t-1)}^s + \sum_{d \in D} x_{dir}^s \right) - y_{int}^s \quad \forall i \in I, r \& t \in T \mid r < t, s \in S \quad (35)$$

4. Resiliency strategy formulations

In this section, resilience-seeking constructs are formulated and then appended to the core model above to enhance the resiliency of the solutions. Here four strategies extracted from the literature are considered, namely, multiple-sourcing, fortification, backup supplier and capacity expansion. With multiple-sourcing, retailers are no more single sourced but are assigned to more than one DC. Fortification refers to strengthening and protecting the facilities against the potential disruptions in order to reduce its severity (ex: ISO 22000). Relying on a backup supplier is another strategy that induces an extra facility, external to the network, is mandated to serve as back-up in case of disruption. The capacity expansion is the fourth strategy which involves the allocation of additional capacity buffers at some identified critical nodes of the network. Hereafter, each of these strategies is further explained and its corresponding formulation to integrate to the core model above is presented.

4.1. Multiple sourcing

An important aspect of this problem is to allow multiple-sourcing. In other words, a retailer may source its needs from multiple DCs proactively when the primary DC cannot support its orders. This is inspired by the work of [Snyder et al. \(2006\)](#) and [Klibi & Martel \(2012a\)](#). In this regard, ψ is defined as the sourcing level parameter. For instance, a value equal to two refers to a double sourcing strategy. This strategic assignment decision is defined in the first stage, and remains the same for all periods and scenarios. Accordingly, [Constraint \(5\)](#) in the core model is modified as follows.

$$\sum_{d \in D} A_{id} = \psi \quad \forall i \in I \quad (36)$$

4.2. Fortification

The idea behind this formulation is to augment capacity resistance against disruptions. Investing in this proactive strategy can help preemptively avoid unforeseen safety threats and allow faster response to any potential disruption. Especially in the food supply chain context, this becomes a vital component for enabling effective food safety and compliance initiatives to help prepare both producers and distributors for potential product recalls. In fact, many standards and regulations are imposed by governments on food companies. [Hasani & Khosrojerdi \(2016\)](#) recently considered fortification formulation, but with a simplistic modeling of disruptions (i.e., without impact and recovery functions). Hereafter, we assumed that fortification level is not limited by a set of discrete protection levels, but is continuous, relying on investment cost, which could lead, eventually, to more precise solutions. To apply this strategy, fpm_{pt}^s , fdm_{dt}^s and fim_{it}^s are defined as the fortification variables of PCs, DCs and retailers, respectively, at period t and under scenario s . The capacity constraints are changed as follows to integrate fortification opportunity.

$$\sum_{d \in D} \sum_{r \in T} x_{pdr}^s \leq (1 - \zeta_{pt}^s + fpm_{pt}^s \zeta_{pt}^s) \left(\sum_n cap_{pn} L_{pn} \right) \quad \forall p \in P, t \in T, s \in S \quad (37)$$

$$\sum_{i \in I} \sum_{r \in T} x_{dir}^s \leq (1 - \zeta_{dt}^s + fdm_{dt}^s \zeta_{dt}^s) \left(\sum_k cap_{dk} L_{dk} \right) \quad \forall d \in D, t \in T, s \in S \quad (38)$$

$$\sum_{r \in T} I_{irt}^s \leq (1 - \zeta_{it}^s + fim_{it}^s \zeta_{it}^s) cap_i \quad \forall i \in I, t \in T, s \in S \quad (39)$$

$$0 \leq fpm_{pt}^s \leq 1 \quad \forall p \in P, t \in T, s \in S \quad (40)$$

$$0 \leq fdm_{dt}^s \leq 1 \quad \forall d \in D, t \in T, s \in S \quad (41)$$

$$0 \leq fim_{it}^s \leq 1 \quad \forall i \in I, t \in T, s \in S \quad (42)$$

According to the above constraints, fortification variables impact the capacity and inventory in the opposite direction of disruption impact. These variables take values between 0 and 1, and are multiplied by the disruption impact when a given facility is hit. Similar changes are applied for inventory constraints.

$$\left(1 - \zeta_{pt}^s + fpm_{pt}^s \zeta_{pt}^s\right) Pr_{pt}^s = I_{prt}^s + \sum_{d \in D} x_{pdr}^s \quad \forall p \in P, r \in R, t \in T, s \in S \quad (43)$$

$$I_{prt}^s = \left(1 - \zeta_{pt}^s + fpm_{pt}^s \zeta_{pt}^s\right) I_{pr(t-1)}^s - \sum_{d \in D} x_{pdr}^s \quad \forall p \in P, r \in R, t \in T, s \in S \quad (44)$$

$$\left(1 - \zeta_{dt}^s + fdm_{dt}^s \zeta_{dt}^s\right) \sum_{p \in P} x_{pdr}^s = I_{drt}^s + \sum_{i \in I} x_{dir}^s \quad \forall d \in D, r \in R, t \in T, s \in S \quad (45)$$

$$I_{drt}^s = \left(1 - \zeta_{dt}^s + fdm_{dt}^s \zeta_{dt}^s\right) \left(\sum_{p \in P} x_{pdr}^s + I_{dr(t-1)}^s\right) - \sum_{i \in I} x_{dir}^s \quad \forall d \in D, r \in R, t \in T, s \in S \quad (46)$$

$$\left(1 - \zeta_{it}^s + fim_{it}^s \zeta_{it}^s\right) \sum_{d \in D} x_{dir}^s = I_{irt}^s + y_{irt}^s \quad \forall i \in I, r \in R, t \in T, s \in S \quad (47)$$

$$I_{irt}^s = \left(1 - \zeta_{it}^s + fim_{it}^s \zeta_{it}^s\right) \left(\sum_{d \in D} x_{dir}^s + I_{ir(t-1)}^s\right) - y_{irt}^s \quad \forall i \in I, r \in R, t \in T, s \in S \quad (48)$$

Also, the associated cost could be as follows which should be added to the objective function (Equation (6)).

$$\sum_{i \in T} \sum_{p \in P} fpm_{pt}^s \zeta_{pt}^s \left(\sum_n cap_{pn} L_{pn}\right) + \sum_{i \in T} \sum_{d \in D} fdm_{dt}^s \zeta_{dt}^s \left(\sum_k cap_{dk} L_{dk}\right) + \sum_{i \in T} \sum_{i \in I} fim_{it}^s \zeta_{it}^s cap_i \quad (49)$$

4.3. Backup supplier

The idea behind this formulation is to specify the backup supplier to be used when the established PCs cannot supply the orders. A backup supplier as a super facility (Benaïcha and Hadj-Alouane, 2013) ensures that the flow of material is maintained if disruption happens to the main sources of the network (Kamalahmadi & Parast, 2017). In this case, when a primary PC is not able to support the downstream demand, inventory in the backup supplier will be transported to DCs to make up for unavailable suppliers. Here, it is assumed that the overall unit procurement cost (purchasing plus transportation costs) from the backup suppliers is higher than normal supply cost from established PCs due to the urgent nature of this recourse. Accordingly, the decision that needs to be integrated to the core model is the amount of product that is provided by the backup supplier and transported to a given DC d in period t under scenario s (denoted by Bu_{dt}^s). Therefore, Equation (11) should be modified as follows.

$$Bu_{dt}^s + (1 - \zeta_{dt}^s) \left(\sum_{p \in P} x_{pdr}^s\right) = I_{drt}^s + \sum_{i \in I} x_{dir}^s \quad \forall d \in D, r \in T, t \in T \mid r = t, s \in S \quad (50)$$

The associated unit cost is production and transportation cost (b_d) from backup suppliers to DCs. So, the cost term to add to [objective function \(6\)](#) is as follows.

$$\sum_{d \in D} \sum_{t \in T} b_d Bu_{dt}^s \quad (51)$$

4.4. Capacity expansion

The last resiliency strategy introduces to the core model is the capacity expansion feature. In this case, facilities have the option to enhance their capacity temporarily in case of disruptions thanks to a capacity buffer available to engage. In this regard, variables $Ce1_{pt}^s$, $Ce2_{dt}^s$ and $Ce3_{it}^s$ are defined to fix the amount of capacity expanded for each period, for PCs, DCs and retailers, respectively. [Equations \(27\)-\(29\)](#) should be modified in the core model as follows.

$$\sum_{d \in D} \sum_{r \in T} x_{pdrt} \leq (1 - \zeta_{pt}^s) \left(\sum_n cap_{pn} L_{pn} \right) + Ce1_{pt}^s \quad \forall p \in P, t \in T, s \in S \quad (52)$$

$$\sum_{i \in I} \sum_{r \in T} x_{dir} \leq (1 - \zeta_{dt}^s) \left(\sum_k cap_{dk} L_{dk} \right) + Ce2_{dt}^s \quad \forall d \in D, t \in T, s \in S \quad (53)$$

$$\sum_{r \in T} I_{irt} \leq (1 - \zeta_{it}^s) cap_i + Ce3_{it}^s \quad \forall i \in I, t \in T, s \in S \quad (54)$$

In addition, capacity expansions impose cost factors on the objective function. $CC1_{pt}$, $CC2_{dt}$ and $CC3_{it}$ are defined as unit capacity expansion costs which will result in the following cost term in the objective function.

$$\sum_{p \in P} \sum_{t \in T} CC1_{pt} Ce1_{pt}^s + \sum_{d \in D} \sum_{t \in T} CC2_{dt} Ce2_{dt}^s + \sum_{i \in I} \sum_{t \in T} CC3_{it} Ce3_{it}^s \quad (55)$$

5. Solution Approach

The two-stage stochastic multi-period design model developed in this work is clearly difficult to solve. This is mainly due to the combinatorial nature of the problem and the high number of scenarios needed to produce good quality solutions ([Klibi and Martel, 2012a](#)). Its complexity is augmented here by the explicit inclusion of the resiliency-seeking equations and the disruption process modeling. Accordingly, this work proposes an efficient solution approach that starts by sampling the set of scenarios and using scenario reduction technique. Next, it considers Benders decomposition (BD) approach to solve the equivalent deterministic problem and speed up the solution time.

5.1. Scenario reduction method

Scenario reduction and sampling methods aim at reducing the number of scenarios in such a way that the reduced numbers can be representative of the entire scenarios set. The k -means clustering method and the fuzzy clustering method (FCM) (Bezdek, 1974) are known approaches used to partition a given number of scenarios with similar features into a predefined number of clusters in order to reduce the number of representative scenarios.

First, a Monte Carlo sampling method is developed in this work to generate plausible future scenarios occurring along the planning horizon. It uses pseudo-random numbers and the inverse of the parameters' distribution function of the random variables involved. Based on the epidemic disruption process described in Section 3.2, the following steps are applied in the proposed Monte Carlo procedure. First, disruption arrival time is generated for each zone based on exponential distribution function. Thus, a chronological list of disruption occurrence is constructed for each zone. Next, for each event in the list, disruption intensity is calculated. Subsequently, a hit test is done for each node in the disrupted zone. In this step, a chronological list of disruption occurrence is constructed for each node of the network. In the fourth step, propagation of disruption and its time lag in the network is adapted based on distance and relations between nodes, and the contaminated nodes and disruption time periods are obtained. Therefore, in this step, the nodes' chronological disruption list is updated. Fifth, time to recovery is calculated for each disrupted node within a function $g_t(\beta_e^s, \theta_e^s)$. Finally, this function is then embedded in the mathematical model via ζ_{et}^s impacting the capacity and inventory levels through the planning horizon. The detailed procedure is given in Appendix A. Note that this procedure generates also realizations of the random demand per retailer per time period. The output of the procedure that is projected in the model is given by variables d_{it}^s for all e, i, t and s . Running the procedure for N times yields a sample of independent and equiprobable scenarios $\{s_1, s_2, \dots, s_n, \dots, s_N\} = S_N$, with $p(s) = 1/N$. Next, scenarios are clustered by means of an FCM that is known to be efficient and straightforward. Next, scenarios placed in a cluster, are substituted by their corresponding cluster center, which is an existing scenario. In traditional clustering methods, each scenario is restricted to belong to only one of the clusters, while FCM eliminates this restriction and adds flexibility through membership degrees. In this method, each object belongs to each cluster with a membership degree that falls between zero and one and is generated randomly at the starting point of the algorithm. It should also be noted that the summation of the membership degrees of a scenario must be equal to one. FCM implementation steps are presented in Appendix A. Applying this method yields M clusters and so M scenarios as representative of the entire N scenarios ($\{s_1, s_2, \dots, s_M\} = S_M \subseteq S_N$). Thus, probability of s_m is equal

to summation of probability of scenarios belonging to cluster m as $p(s_m) = \sum_{n|n \in m} p(s_n)$ which is also equal to $|s_m|/N$ where $|s_m|$ indicates cardinality of scenarios in cluster m . Accordingly the objective function (1) must be adapted to consider the sampled scenarios. When applying the FCM, the objective function must be rewritten as follows:

$$\text{Max } Z = \sum_{s_m \in S_M} p(s_m) Q(\mathbf{x}, s_m) - \sum_{p \in P} \sum_{n \in N} f_{pn} L_{pn} - \sum_{d \in D} \sum_{k \in K} f_{dk} L_{dk} \quad (56)$$

5.2. Benders decomposition algorithm

The problem introduced in Section 3 is a very complex mixed-integer problem since it includes a high number of integer variables. Its structure is well-suited for a decomposition approach such as Benders decomposition (BD) (Benders, 1962). In addition, benefiting from the merits of cutting plane acceleration can be appropriate (Santoso et al., 2005). In BD, instead of solving the complex MIP problem, the problem is decomposed into a pure integer problem and a linear problem, which are called master and sub-problems, respectively. These two problems are solved iteratively by using the solution obtained from each other until the termination condition is achieved. We first briefly present the general version of this approach, and then we explain a number of acceleration techniques which are applied to enhance the performance of the proposed BD. A detailed formulation is provided in Appendix B.

In order to develop a BD algorithm for the mathematical model concerned (1) - (25), the dual sub-problem (DSP) and master problem (MP) should be formulated. To make the work more convenient, we consider the general model presented in Section 3. Let us fix the integer variables to given fixed values ($L_{pn} = \bar{L}_{pn}$, $L_{dk} = \bar{L}_{dk}$, $A_{id} = \bar{A}_{id}$). The Benders primal sub-problem (PSP) is then formulated as in Appendix B. The DSP should now be formulated, providing a lower bound for the objective function of the original problem at each iteration because this is a maximization problem. Let dv^* represent the dual variables of the constraints of the formulated PSP, then, the DSP is formulated as in Appendix B. According to the DSP solution, the MP provides an upper bound for the objective function of the original model at iterations of the algorithm. The MP is also presented in Appendix B. The BD algorithm in its general form may require a large number of iterations and computational time to become converged. Thus, in order to improve the convergence of the BD algorithm, some acceleration techniques adopted from the literature are employed.

First, valid inequalities can boost convergence of the BD algorithm by adding constraints based on information useful to MPs (Cordeau et al. 2006, Pishvaei et al., 2014). Low quality MP solutions could result in slow convergence of the algorithm. Here, on the basis of minimum demand satisfaction and according to Constraint (18), two valid inequalities can be added to the MP as follows. These two constraints ensure that the capacity of the established PCs and DCs satisfy the minimum demand level. Consequently, adding these inequalities to the MP restricts the feasible region and prevents insufficient establishment of the PCs and DCs. The primary iteration of the algorithm will therefore be improved in terms of initial upper bound.

$$\sum_{p \in P} \sum_{n \in N} cap_{pn} L_{pn} \geq \sum_{i \in I} \sum_{t \in T} d_{it} \quad (57),$$

$$\sum_{d \in D} \sum_{k \in K} cap_{dk} L_{dk} \geq \sum_{i \in I} \sum_{t \in T} d_{it} \quad (58)$$

Second, a disaggregation method is applied to the PSP. This method was first introduced by Dogan & Goetschalckx (1999) for a multi-period production distribution problem in order to restrict MP solution and consequently speed up convergence. Thereafter, this technique was employed for solving complex network problems (Pearce & Forbes, 2018). In this technique, the primal sub-problem is decomposed into the independent sub-problems, again through which an optimality cut is achieved. In our case, we decompose the PSP into S sub-problems such as each scenario is considered to be a sub-problem which has its corresponding DSP as DSP^s . Figure 6 summarizes the general BD and the acceleration techniques employed to solve the set of models above.

We note that the big M parameter used in Constraints (7) and (8) was bounded by the maximum amount of product to be transferred inside the network ($\sum_{i \in I} \sum_{t \in T} d_{it}$), to enhance the initial lower bound of the problem.

<p>Step1. Set $LB = -\infty$ and $UB = +\infty$</p> <p>Step2. Set $L_{pn} = 1, L_{dk} = 1$ and $A_{di} = 1$ as an initial feasible value for binary variables</p> <p>Step3. Solve the disaggregated dual sub-problems to find the optimal value of dual variables (dv_{\circ}°)</p> <p>Step4. If $LB < DSP^{s1} + \dots + DSP^S + \text{constant}$ then $LB = DSP^{s1} + \dots + DSP^S + \text{constant}$.</p> <p>Step5. Form the master problem by adding optimality and feasibility cuts.</p> <p>Step6. Solve the master problem and set $UB = MSP$</p> <p>Step7. If $UB - LB < \varepsilon$, then stop the algorithm and report the obtained solution and relevant objective function value; otherwise, go to step 3.</p>

Figure 6 Proposed BD algorithm based on acceleration techniques

6. Experimental results

In this section, the proposed RFSCND model as well as the variants including the resiliency constructs are tested on a bench of problem instances realistically designed. The corresponding numerical results are analyzed and discussed via extensive viewpoints.

6.1. Experimental plan

The business case considered here is related to a company in the food sector that aims to deploy a resilient national production-distribution network. To this end, five candidate locations are considered for establishing PCs, which are fed by global suppliers and where for each PC three capacity levels are available. Next, ten potential locations for DCs are considered, with three capacity levels per DC. Finally, fifteen retail points are defined to complete the network. The horizon plan is one year and is composed by 26 biweekly time periods. Our preliminary tests shown that with a biweekly time period we are able to capture the essence of the planning decisions as well as the propagation of the epidemic disruptions. The lead time between PCs and DCs and between DCs and retailers is less than a time period (i.e., zero lead time). Scaled parameters of the considered case are according to the values specified in Table 2. Three capacity levels of (7500, 8500, 10000) and (3500, 5000, 7000) throughput units, are considered for PCs and DCs per time period, respectively.

Table 2 Parameters values

Processing Centers			Distribution Centers			Retailers		
Parameter	Value	Unit	Parameter	Value	Unit	Parameter	Value	Unit
f_{pn}	$U(60000, 80000)$	€	f_{dm}	$U(35000, 60000)$	€	h_i	$U(0.4, 0.9)$	€/Period
c_{pd}	$U(0.02, 0.35)$	€/Mile	c_{di}	$U(0.04, 0.47)$	€/Km	ω_{it}	$U(8, 14)$	€/unit
c_p	$U(1.6, 1.8)$	€	h_d	$U(0.1, 0.8)$	€/Period	d_{it}^s	$U(0.1, 0.8)$	Unit
h_p	$U(0.1, 1.5)$	€/Period	ce_{dt}	$U(0.4, 1.1)$	€/unit	ce_{it}	$U(0.4, 1.1)$	€/unit
ce_{pt}	$U(0.4, 1.1)$	€				ls_{it}	$U(4, 7)$	€/unit
sl	3	Period						

From this baseline network, three key dimensions are varied in our experiments: capacity level $\{Cap^{low}, Cap^{high}\}$, shelf life $\{SL^{low}, SL^{high}\}$ and lost-sale cost $\{ls^{low}, ls^{high}\}$. The Cap^{low} is 15% less than the nominal capacity levels and Cap^{high} is 15% higher. The shelf-life of product is randomly generated in intervals [1, 2] and [4, 6] for SL^{low} and SL^{high} , respectively. Also, ls^{low} and ls^{high} lost-sales values are varied in intervals [0.5, 1.5] and [5, 8], respectively. From Table 2, it is assumed that inventory holding costs are fixed and not product's age dependent. The mentioned dimensions are tested under six strategies: risk avoidance (**Ra**) when no resiliency construct is applied, backup

suppliers (**Bs**), fortification (**Fo**), multiple-sourcing (**Ma**), capacity expansion (**Ce**) and risk ignorance (**Ri**) when disruptions are ignored. A combination of the three varying dimensions and six design models yielded 48 problem instances.

For a given scenarios sample, solving each proposed model produces a network design solution, denoted by \mathbf{Y}^j ; $j=1, \dots, J$. Each obtained network design specifies the set of PCs and DCs to open with specified capacity level and assignment decisions of retailers to the opened PCs. In addition to these decisions, each model produces its resiliency-seeking policy that needs to be considered from the strategic level in terms of additional assignments to cover the retailers or additional capacity level/buffer to hedge the inventories. More specifically, the **Ma** model determines the multiple-sourcing policy and thus specifies which the primary and secondary assignments for each retailer are. The **Bs** model provides the instruction on the backup supply sources to have and total expected amount of product that could be procured from them. The **Ce** model provides the total amount of expandable capacity that is at the disposal of the network as a contingency plan. In the same way, the **Fo** model provides the total amount of capacity recovery that could be mitigated thanks to the investments in DCs fortification. To evaluate these alternative designs, their respective decisions vectors \mathbf{Y}^j ; $j=1, \dots, J$ are assessed using a much larger set of scenarios, denoted by \mathcal{S}_N . To do so, a comprehensive inventory-flow model is used that is based on the core second-stage model (6)-(25) appended with constraints (37)-(48), (50) and (52)-(54) and terms (49), (51) and (55) in the objective function. This evaluation model is separable per scenario and this allows considering a larger set of scenarios and also computing additional performance measures. For a given design j , the evaluation of the second-stage model is used to compute the total profit during the planning horizon, under a given scenario, that is $\hat{Z}(\mathbf{y}^j, s)$; $\forall j \in J, s \in \mathcal{S}_N$, and thus the summation over \mathcal{S}_N , provides the expected value. Here, $\hat{Z}(\mathbf{y}^j, s)$ indicates the total profit earned through the terms of the objective function of the core model (1) in addition to the terms (49), (51) and (55). Besides the total expected profit, the expected fill rate and the expected product freshness are assessed. In FSCs, inventory velocity and supply speed are key performance indicators that show continuity of product flow through the network. In this study, these are reflected in product age and its price as special characteristics of FSCs. These two indicators can be calculated as given in Equations (59) and (60). According to Equations (60), freshness index is always a positive real number. The less value of this index indicates the fresher products are delivered to consumers.

$$\text{Expected Fill Rate} = \frac{1}{N} \sum_{s \in S_N} \left(\frac{\sum_{i \in I} \sum_{r \in T} \sum_{t \in T} y_{irt}^s}{\sum_{i \in I} \sum_{t \in T} d_{it}^s} \right) \quad (59)$$

$$\text{Expected Product Freshness} = \frac{1}{N} \sum_{s \in S_N} \left(\frac{\sum_{i \in I} \sum_{r \in T} \sum_{t \in T} |t - r| y_{irt}^s}{\sum_{i \in I} \sum_{r \in T} \sum_{t \in T} y_{irt}^s} \right) \quad (60)$$

Finally, to measure the risk exposure related to the design solution in establishing PCs and DCs in risky locations, another indicator is considered. Let $\gamma(\mathbf{Y}^j, s)$ be the total number of disruptions on established facilities under scenario s when design \mathbf{Y}^j is implemented. Thus, the average number of hits for a given design \mathbf{Y}^j and set of scenarios can be calculated through Equation (61).

$$\bar{\gamma}(\mathbf{Y}^j) = \left(\sum_{s \in S_N} \gamma(\mathbf{Y}^j, s) \right) / |S_N| \quad (61)$$

6.2. Computational Results

This subsection presents the computational results based on the performance of the FCM algorithm and the BD approach. To implement the FCM algorithm and generate a large sample of scenarios with Monte Carlo procedure (Figure A.1) MATLAB R2015b software was used. FCM algorithm cluster scenarios based on two attributes: number of hits and total amount of lost capacity in the whole network. This partitioning is based on the rational that the plausible future scenarios generated with the Monte-Carlo procedure may involve variable levels of risk, which can be measured by the number of hits it undergoes during the planning horizon. Accordingly, Figure 7 illustrates the distribution of the number of hits for a large sample of scenarios that are categorized into 10 clusters with exponential inter-arrival times. As depicted, some scenarios involve only few disruptions over the planning horizon but others may be much more chaotic as they involve several hits. Recall that the number of hits depicted here is associated to the potential network (i.e. including all the potential PCs and DCs), over the planning horizon.

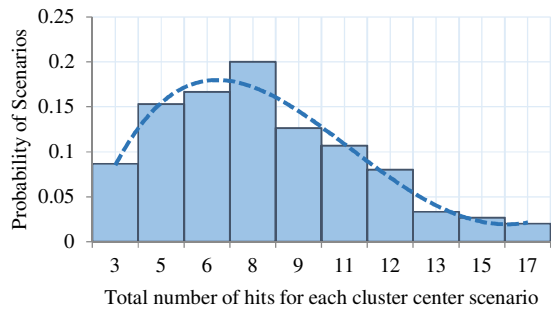


Figure 7 Scenario clustering for a large sample scenario

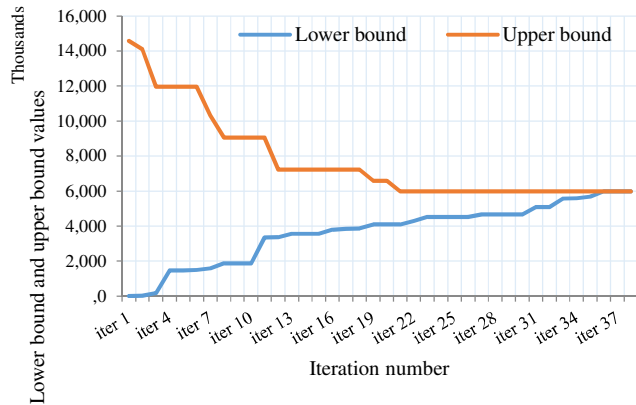


Figure 8 The convergence progression of the BD algorithm

Another important feature of the solution approach is the BD developed to enhance the solvability of the design models proposed. This algorithm is coded in GAMS 24.1.3 optimization software, with CPLEX 11.2 solver used to solve the linear DSP and integer MP. The experiments are run on a machine with a 1.7 GHz processor and 4GB of RAM. In this section the computational efficiencies achieved by implementing BD and adding accelerating methods are measured in terms of algorithm iterations and computational times. In addition to the baseline network, three other instances with augmented problem-size are tested (i.e., increased number of PCs, DCs and retailers). The characteristics of the test instances are presented in Table 3. This table also presents the performance of the solution approach, where the stopping criteria are (a) maximum of 150 Benders iterations and (b) optimality gap below threshold 0.1. As the experimental results indicate, the proposed accelerated BD algorithm is significantly more time-efficient compared to the CPLEX 11.2 solver. According to these results, it can be claimed that the proposed BD algorithm is worthy to develop as it allows solving realistic sizes of the FSC design problem. The visual representation of the BD algorithm convergence is provided at Figure 8 for the instances number 4 of Table 3.

Table 3 Comparative progression results among proposed BD algorithm and CPLEX

Instance	$ P $	$ D $	$ I $	$ T $	$ S $	Number of variables	Number of constraints	Accelerated BD		CPLEX Time(s)
								Number of Iterations	Time(s)	
1	2	3	5	5	3	1,785	3,205	3	50	1,202
2	4	5	8	10	5	36,422	70,702	8	60	3,650
3	5	8	15	15	8	137,076	385,107	19	1,300	18,376
4 (Studied Case)	5	10	20	26	10	720,445	2,299,935	37	2,677	98,260

6.3. Analysis of Results

Given the 48 problem instances specified previously, this section discusses the quality of the proposed network designs using the set of performance measures. Table 4 provides comparative results on the performance of the

resiliency strategies by performance measure, given by problem-instance. It is worth mentioning that the different models built never produce the same network design. According to this table, **Bs** and **Fo** designs dominate **Ma** and **Ce** designs. **Fo** design solutions perform better when the capacity of the facilities is larger since this disruptions-mitigation strategy acts directly on fortifying the capacities. For instance, in $(Cap^{low}, -, -)$ instances, **Bs** overcomes the **Fo** design solution (a gap of 4.8% in expected profit : 4,370,726€ versus 4,160,931€, respectively) , however the opposite behavior was observed in $(Cap^{high}, -, -)$ instances. For instance, in $(Cap^{high}, SL^{low}, Js^{low})$ instance, **Fo** provides an expected profit of 6,364,570€ which is 6.3% better than **Bs**, 15.8% better than **Ma**, and 25% better than **Ri**. As another viewpoint, in $(Cap^{low}, -, -)$ the expected profit of all the design models are very sensitive to lost-sales cost but it is reduced for $(Cap^{high}, -, -)$ instances. As for the fill rate, the performance and behavior of the design solutions is the same as their profit. For instance, under high capacity, the fill rate exceeds 90% only for **Bs** and **Fo** designs, is relatively close for **Ma** and **Ce** (89.5%), but drops critically for **Ra** (77.6%) and **Ri** (67.4%). When it comes to product freshness, the calculated index shows that **Fo** design performs better than all the other designs in most of the cases with values closed to zero (ranging from 0.117 to 0.006). For instance, a freshness index of 0.117 indicates that about 88% of the products delivered to customers were produced within the last two weeks. Furthermore, the results indicate that **Ri** design is extremely vulnerable in the presence of epidemic disruptions, especially in $(Cap^{low}, -, -)$ instances. The expected profit and fill rate are clearly lower (by 68% and 44%, respectively) compared to the best designs produced because the exclusion of disruption scenarios from the second-stage and thus the removal of recourse decisions/costs, lead to the opening of risk-exposed facilities, which is congruent with the findings in [Klibi and Martel \(2012a\)](#).

It can be concluded that under high capacities, total expected profit and expected fill rate are better and it is because the network is pushed to build buffers without paying any extra charges for it. Although buffers in turn cause a decrease in the expected freshness, the model prevents lost sales to achieve higher profits, which can be interpreted as the “free resilience”. Also, as a general conclusion for all the designs, in $(-, SL^{high}, -)$ instances, the freshness rate is a little decreased since the model can keep inventory for future deliveries as an inherent response to disruptions. Thus, it is a clear tradeoff performance to reach between the expected fill rate and the expected product freshness.

Table 4 Model's performance under different dimensions and in terms of indicators

	$(Cap^{low}, SL^{low}, Js^{low})$	$(Cap^{low}, SL^{low}, Js^{high})$	$(Cap^{low}, SL^{high}, Js^{low})$	$(Cap^{low}, SL^{high}, Js^{high})$	$(Cap^{high}, SL^{low}, Js^{low})$	$(Cap^{high}, SL^{low}, Js^{high})$	$(Cap^{high}, SL^{high}, Js^{low})$	$(Cap^{high}, SL^{high}, Js^{high})$
Expected profit gap from the best in %								
Ra	-30.4	-59.1	-30.3	-58.3	-17.8	-25.2	-17.2	-24.3
Bs	0	0	0	0	-6.3	-9.5	-5	-6.7
Fo	-4.8	-9	-5.1	-9.6	0	0	0	0

<i>Ma</i>	-30	-58	-29.9	-57.3	-15.8	-21.7	-15.6	-21.4
<i>Ce</i>	-24	-49.9	-24.3	-49.7	-12.1	-18.1	-12	-17.8
<i>Ri</i>	-43	-68	-43	-68	-25	-33	-25	-33
Expected fill rate (%)								
<i>Ra</i>	62.6	62.6	62.6	62.6	77.6	78.2	88	88
<i>Bs</i>	79.3	79.3	79.3	79.3	92.6	92.6	93.9	94.2
<i>Fo</i>	75.1	75.1	75.1	75.1	94.6	94.6	95.6	95.6
<i>Ma</i>	64.6	64.6	64.6	64.6	89.5	89.5	89.5	89.5
<i>Ce</i>	64.6	64.6	64.6	64.6	89.5	89.5	89.5	89.5
<i>Ri</i>	56.6	56.6	56.6	56.6	67.4	67.4	67.4	67.4
Expected freshness index								
<i>Ra</i>	0.084	0.252	0.101	0.285	0.083	0.095	0.178	0.221
<i>Bs</i>	0.068	0.083	0.079	0.166	0.087	0.089	0.169	0.190
<i>Fo</i>	0.006	0.048	0.006	0.117	0.006	0.008	0.010	0.012
<i>Ma</i>	0.084	0.199	0.091	0.282	0.053	0.097	0.071	0.127
<i>Ce</i>	0.002	0.111	0.014	0.195	0.053	0.098	0.065	0.124
<i>Ri</i>	0.091	0.251	0.094	0.251	0.088	0.252	0.088	0.254

Table 5 shows the behavior of the design solutions produced with the resiliency-seeking strategies in terms of design decisions. For each alternative design model, the network structure is represented in terms of the average number of opened PCs and DCs among all the instances. The outcomes indicate that the network structures are rarely the same which is congruent with the performance results in Table 4. As expected, *Ra* as the free-resilience design model produces the highest number of opened facilities, which indicates that this network tries to hedge against the risk of disruption with its coverage. *Bs* designs have lower number of opened PCs among the resiliency-seeking strategies since they rely on the external super facility and thus invest less in endogenous resources. Finally, *Ri* designs provide the lowest average number of opened PCs and DCs since the design model seeks efficiency and do not value buffers.

Table 5 Network structure of resiliency seeking design models

	Design models					
	<i>Ra</i>	<i>Bs</i>	<i>Fo</i>	<i>Ma</i>	<i>Ce</i>	<i>Ri</i>
Average # of opened PCs	4	3.44	3.60	4	3.92	3
Average # of opened DCs	7	6.15	5.86	6.25	6.45	5

Moreover, the disruption exposure level of each design solution is presented in terms of average number of disruptive events in Figure 9 (i.e. number of hits on the opened PC and DC locations). It reveals that *Ra* design performs well in this point of view, as expected, since it provides a risk avoidance design. This can be interpreted as the fact that this design is the best one as the natural cover against disruptions but the pay-offs comes with a lower expected profit compared to the other design solutions. On the hand, resiliency-seeking designs are more often in the exposure of disruptions since there is a demand flow for some retailers when they are disrupted. These designs, in top design produced by *Fo* and *Bs* strategies, accept a higher exposure level since they are fortified by resiliency-constructs and contingency plans. In other words, the resiliency-seeking strategies tend to find good trade-offs

between the cost of investing in resiliency and the network profitability thanks to the recourse modeling in the stochastic program. The **Ri** design solutions undergo the highest exposure level.

In the same way, the disruption-profit graph of resiliency-seeking designs is presented in Figure 10 in terms of profit generated under a given number of disruptions. These figures reveal that **Fo** and **Bs** strategies are dominating ones in both low and high capacity levels and show a resilience behavior toward disruptions. **Ma** and **Ce** designs approximately have the same trend which is a resistance only to few disruptions. An interesting point in Figure 10 a) is that when there is not any disruption (i.e, 0 hits), all the strategies have the same profit except **Bs**, which means connecting the network to a super facility could be profitable when we are operating only with stochastic demand quantities. While in ($Cap^{high}, -, -$) instances, all the design solutions are equal at zero hits, and thus the super facility doesn't provide any advantage to support the demand level. When the capacity level is low, the profit value is dramatically decreased with increasing number of disruptive events. That is because the propagation probabilities are intensifying the severity of disruptions and this becomes more affecting. In case of high capacity level, the propagation severity could be absorbed to some extent. In ($Cap^{high}, -, -$) instances (Figure 10b) and for low- and medium-risk scenarios (less than 8 disruptions), **Fo**-design model tends to give higher profits. However, for high-risk scenarios **Bs**-design model create more profit thanks to the presence of the super facility.

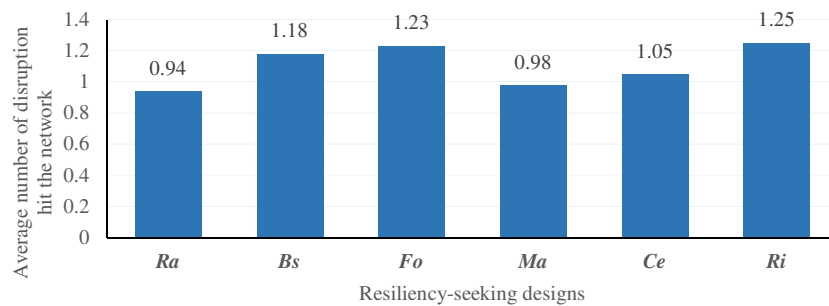


Figure 9 Average numbers of disruptions for each design

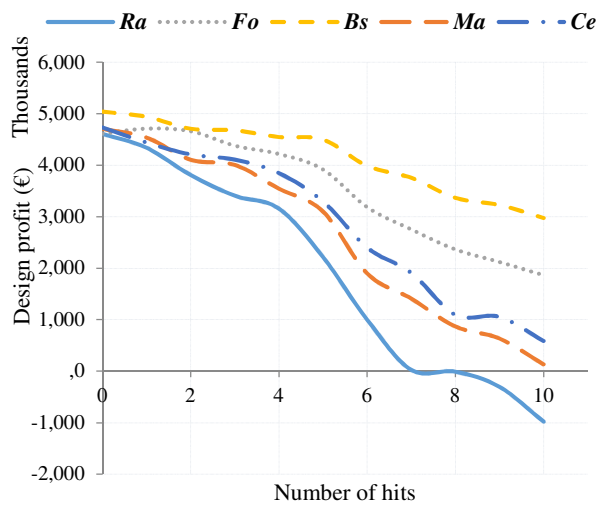


Figure 10 a) Disruption-profit graph of resiliency seeking designs for $(Cap^{low}, SL^{high}, ls^{low})$

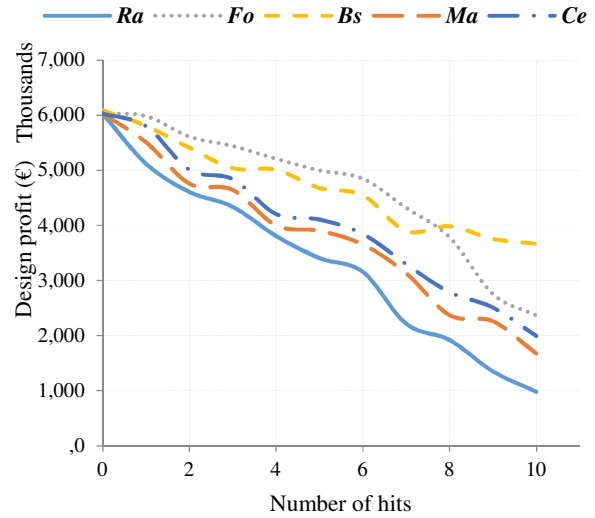


Figure 10 b) Disruption-profit graph of resiliency seeking designs for $(Cap^{high}, SL^{high}, ls^{low})$

Moreover, the pricing strategy, presented in Figure 2, has an important influence on the expected total profit, demand satisfaction and product freshness. Here, a sensitivity analysis is explored by three pricing strategies. According to Figure 11, first and second price types are fixed and equal to 8 and 14 respectively, and the third price type is an age-varying pricing ranging from 8 to 14. Figure 11 reveals that increasing the selling price implicitly leads to higher profit levels. However, comparing fixed price to 14 and age-varying price reveals that although objective functions are approximately equal, demand satisfaction, product freshness and inventory holding cost are considerably lower in the case of the variable price. It can be concluded that the production-distribution system tries to maximize the freshness of the consumed products to earn more profit and hold less inventory because this increases product's age. This behavior underlines the crucial importance in FSCs to model adequately the pricing strategy in link with products freshness and age as done in this paper with the age-varying price.

In this last part, we have considered different levels of resiliency budget to analyze how the design solutions behave. Before applying any resiliency strategy, the objective function in the case of disruption and no-disruption are fixed in Figure 12b). According to this figure, resiliency strategies have considerable impact on the design solution. Given the resiliency strategies, the objective function is increased to $5,843 \times 10^3$. This increase trend is up to 120,000 in budget, and a budget of more than this does not significantly change the objective function. Thus, it can be concluded that in the considered case, resiliency strategies and a budget of 120,000 could result in higher profits for this FSC. On the other hand, resiliency strategies consume different portions from the allocated budget, as shown in

Figure 12a). As expected, fortification and backup supplier strategies consume more of the allocated budget than capacity expansion. Additionally, as the allocated budget increases, the portion of backup supplier definitely increases, while the capacity expansion amount fluctuates and does not fit a specific trend.

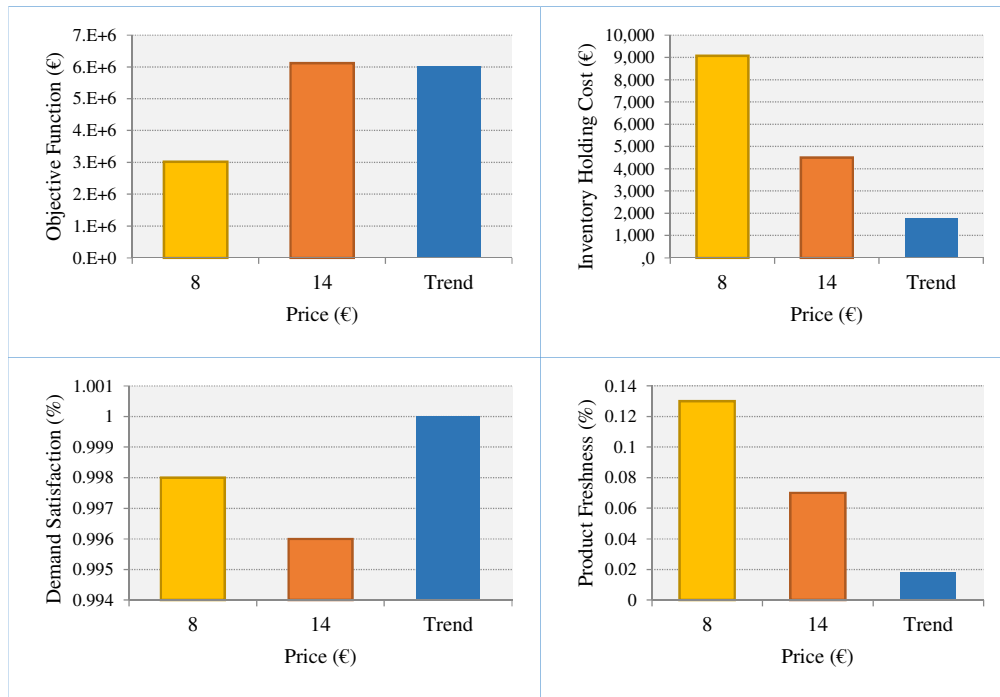


Figure 11 Sensitivity analyses on pricing method

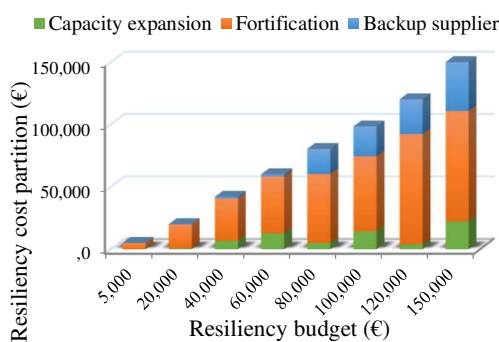


Figure 12a) Cost details according to resiliency budget

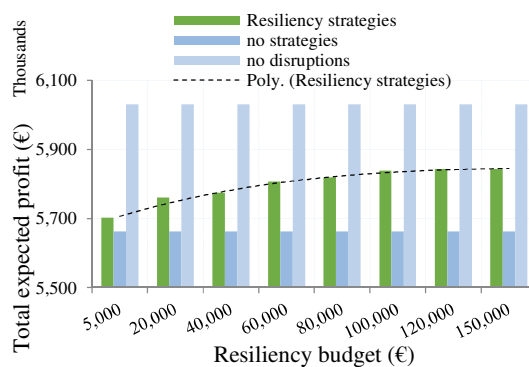


Figure 12b) Sensitivity analyses on resiliency budget

Although resiliency strategies were mainly developed to tackle the disruptions with low probabilities and big impacts, here they are used to deal with uncertainty degree of demand regardless of disruptions. Therefore, three categories are assumed for demand process based on the mean and standard deviation for each demand type. These

types are namely: deterministic demand (**DT1**), where demand of each retailer is constant over the planning horizon; stochastic stationary demand (**DT2**), where the demand of each retailer follows a distribution function whose parameters are constant over the planning horizon; stochastic non-stationary demand (**DT3**), where unlike **DT2**, the distribution parameters not constant, but varying over the planning horizon.

In Table 6, comparative results on the performance of the resiliency-seeking designs are provided regarding the three demand types. Here low-capacity instances are selected for analysis to ignore the free-resilience of the model and highlight the various design impacts. Obtained results indicate that overall there is a decrease in the three indicators of the networks for all design models, as demand uncertainty is increased. This negative growth is amplified in *Ra* design since it is not supported by any of the resiliency strategies. It is worth mentioning that here for all three demand types, the *Fo* design behaves exactly same as the *Ra* design. It was expected since the fortification design plays role just in case of disruptions it is not activated for demand changes. Unlike disruption uncertainty case, the *Bs*, *Ma* and *Ce* designs lead to indicators with negligible differences. However, they could enhance the networks performance compared to the *Ra* design. Furthermore, *Ri* dominates *Ra* design since in *Ri* design demand points are closely covered when ignoring the disruption occurrence, while *Ra* uses free-resiliency design that leads to a low-density network in which the transportation costs are considerable.

Table 6 Impact of resiliency-seeking designs on tackling the demand uncertainty

	Expected Profit			Expected Freshness			Expected Fill Rate		
	DT1	DT2	DT3	DT1	DT2	DT3	DT1	DT2	DT3
<i>Ra</i>	5,638,470	5,230,087	4,908,421	0.002	0.014	0.057	0.961	0.912	0.840
<i>Bs</i>	5,639,029	5,233,546	4,915,116	0.002	0.008	0.016	0.965	0.930	0.897
<i>Fo</i>	5,638,470	5,230,087	4,908,421	0.002	0.014	0.057	0.961	0.912	0.840
<i>Ma</i>	5,638,521	5,232,977	4,911,089	0.002	0.009	0.015	0.962	0.930	0.863
<i>Ce</i>	5,638,470	5,231,491	4,910,790	0.002	0.012	0.015	0.962	0.923	0.862
<i>Ri</i>	5,638,953	5,231,474	4,910,331	0.002	0.012	0.057	0.965	0.930	0.880

7. Concluding remarks

Resiliency of food supply chains has become more important in recent years due to increasing vulnerabilities imposed by different aspects of uncertainties, especially epidemics. Systematic design and optimization of FSC networks can significantly assist in pushing further towards efficiency, especially in developing countries. A quantitative approach is used in this paper, to cope with epidemic disruptions which are modeled beside business-as-usual uncertainties through a risk modeling and propagation approach. The framework of stochastic programming

with recourse is employed to incorporate scenarios of epidemics disruptions and to evaluate the expected losses and recourses to be incurred under such events. In addition, a number of resilience strategies are incorporated into the proposed core model to mitigate the impacts of disruptions. Next, an FCM algorithm is deployed that reduces the complexity related to the huge number of disruption scenarios, which is coupled with an accelerated Benders decomposition algorithm. From the experiments made, the established capacity and lost-sale cost are found to be the most influencing factors for the yielded FSC network desirability in terms of profit, fill rate and product freshness such that they could impact resiliency-seeking model selection. Among the resiliency-seeking models, fortification and backup supplier strategies provided more resilient solutions in comparison with multiple-sourcing and capacity expansion. Another key finding is that we observed that age-dependent price instead of fixed product price could have considerable impact on FSC indicators. It is worth mentioning that our risk modeling approach demonstrated that the impact of an extreme event on FSCs not only depends on the arrival rate but on the intensity magnitude, propagation scale and the preparedness level. Designing a resilient FSC by anticipation to yearly and mid-term extreme events clearly helps in providing valuable attributes to the SC in order to durably perform well under various unforeseen scenarios (epidemic outbreaks, pandemics, disasters). The explicit inclusion of these later scenarios necessitates the consideration of longer planning horizons, additional risk data and advanced solution methods.

Several research avenues can be recommended to enrich this promising area of the RFSCND problem. One of the main issues in FSC and especially in cold chains is the emission of hazardous gases like CO₂ and NO_x during transportation and when keeping inventories in refrigerated warehouses. On the other hand, FSCNDs are in the early stages of development in developing countries and they could incorporate social issues. Therefore, addressing sustainability issues in conjunction with resiliency considerations may provide more comprehensive decision tools for decision-makers (DMs) in developing countries. Another interesting idea for future research could be implementing robust scenario-based optimization methods that could incorporate DMs attitudes to risk including risk aversion, risk seeking and neutral into the modeling approach. Another immediate research idea is to explicitly investigate from-farm-to-fork network design problem associated with food traceability issues as another resiliency strategy that would require new modeling techniques. Furthermore, other related resiliency strategies such as technology investment for food traceability is of high interest. The models presented in this paper would be a good starting point for these extensions.

References

- Amiri-Aref, M., Klibi, W. and Babai, M.Z., 2018. The multi-sourcing location inventory problem with stochastic demand. *European Journal of Operational Research*, 266(1), pp.72-87.
- An, K. and Ouyang, Y., 2016. Robust grain supply chain design considering post-harvest loss and harvest timing equilibrium. *Transportation Research Part E: Logistics and Transportation Review*, 88, pp.110-128.
- Azad, N., Saharidis, G.K., Davoudpour, H., Malekly, H. and Yektamaram, S.A., 2013. Strategies for protecting supply chain networks against facility and transportation disruptions: an improved Benders decomposition approach. *Annals of Operations Research*, 210(1), pp.125-163.
- Baghalian, A., Rezapour, S. and Farahani, R.Z., 2013. Robust supply chain network design with service level against disruptions and demand uncertainties: A real-life case. *European Journal of Operational Research*, 227(1), pp.199-215.
- Behzadi, G., O'Sullivan, M. J., Olsen, T. L., Scrimgeour, F., & Zhang, A. (2017). Robust and resilient strategies for managing supply disruptions in an agribusiness supply chain. *International Journal of Production Economics*, 191, 207-220.
- Behzadi, G., O'Sullivan, M.J., Olsen, T.L. and Zhang, A., 2018. Agribusiness supply chain risk management: A review of quantitative decision models. *Omega*, 79, pp.21-42.
- Benaïcha, S. and Hadj-Alouane, A.B., 2013. Super facilities versus chaining in mitigating disruptions impacts. *Computers & Industrial Engineering*, 65(3), pp.351-359.
- Benders, J.F., 1962. Partitioning procedures for solving mixed-variables programming problems. *Numerische mathematik*, 4(1), pp.238-252.
- Bezdek, J.C., 1973. *Fuzzy Mathematics in Pattern Classification*. Cornell University, Ithaca, New York, United States.
- Bortolini, M., Faccio, M., Ferrari, E., Gamberi, M. and Pilati, F., 2016. Fresh food sustainable distribution: cost, delivery time and carbon footprint three-objective optimization. *Journal of Food Engineering*, 174, pp.56-67.
- Bourlakis, M., and P. Weightman. 2004. *Food Supply Chain Management*. Oxford: Blackwell Publishing
- Brende, B. (2019). *The Global Risks Report 2019, 14th Edition*. Geneva: World Economic Forum.
- Chopra, S., Sodhi, M., 2004. Managing Risk to Avoid Supply-Chain Breakdown. *MIT Sloan Management Review*, 46, pp 53.
- Cordeau, J.F., Pasin, F. and Solomon, M.M., 2006. An integrated model for logistics network design. *Annals of operations research*, 144(1), pp.59-82.
- De Keizer, M., Akkerman, R., Grunow, M., Bloemhof, J.M., Haijema, R. and van der Vorst, J.G., 2017. Logistics network design for perishable products with heterogeneous quality decay. *European journal of operational research*, 262(2), pp.535-549.
- Dani, S., & Deep, A. (2010). Fragile food supply chains: reacting to risks. *International Journal of Logistics: Research and Applications*, 13(5), 395-410.
- Dasaklis, T. K., Pappis, C. P., & Rachaniotis, N. P. (2012). Epidemics control and logistics operations: A review. *International Journal of Production Economics*, 139(2), 393-410.
- Dogan, K., Goetschalckx, M., 1999. A primal decomposition method for the integrated design of multi period production–distribution systems. *IIE Transactions*. 31(11), pp.1027–1036.
- Du, B., Zhou, H., & Leus, R. (2020). A two-stage robust model for a reliable p-center facility location problem. *Applied Mathematical Modelling*, 77, 99-114.
- Dupuy, C., Botta-Genoulaz, V., & Guinet, A. (2005). Batch dispersion model to optimise traceability in food industry. *Journal of Food Engineering*, 70(3), 333-339.
- Esteso, A., Alemany, M.M.E. and Ortiz, A., 2018. Conceptual framework for designing agri-food supply chains under uncertainty by mathematical programming models. *International Journal of Production Research*, 56(13), pp.1-29.

- FAO, 2009. The state of agricultural commodity markets 2009. Rome, Italy, Food and Agriculture Organization of the United Nations, pp. 66.
- Fattahi, M., Govindan, K. and Keyvanshokoo, E., 2017. Responsive and resilient supply chain network design under operational and disruption risks with delivery lead-time sensitive customers. *Transportation Research Part E: Logistics and Transportation Review*, 101, pp.176-200.
- Faturechi, R. and Miller-Hooks, E., 2014. Travel time resilience of roadway networks under disaster. *Transportation research part B: methodological*, 70, pp.47-64.
- Goh, M. (1992). Some results for inventory models having inventory level dependent demand rate. *International Journal of Production Economics*, 27(2), 155-160.
- Goh, M., Lim, J. Y., & Meng, F. (2007). A stochastic model for risk management in global supply chain networks. *European Journal of Operational Research*, 182(1), 164–173.
- Goh, M., & Sharafali, M. (2002). Price-dependent inventory models with discount offers at random times. *Production and Operations Management*, 11(2), 139-156.
- Gonzalez, C.: Climate change, food security, and agrobiodiversity: toward a just, resilient, and sustainable food system. *Fordham Env. Law Rev.* 22, 11–19 (2011)
- Grillo, H., Alemany, M.M.E., Ortiz, A. and Fuertes-Miquel, V.S., 2017. Mathematical modelling of the order-promising process for fruit supply chains considering the perishability and subtypes of products. *Applied Mathematical Modelling*, 49, pp.255-278.
- Hasani, A. and Khosrojerdi, A., 2016. Robust global supply chain network design under disruption and uncertainty considering resilience strategies: A parallel memetic algorithm for a real-life case study. *Transportation Research Part E: Logistics and Transportation Review*, 87, pp.20-52.
- Henderson, D.A., 1999. The looming threat of bioterrorism. *Science*, 283(5406), pp.1279-1282.
- Ivanov, D., Dolgui, A., Sokolov, B., 2019. Ripple effect in the supply chain: Definitions, frameworks and future research perspectives. In: *Handbook of ripple effects in the supply chain*. New York, Springer, 1-33.
- Ivanov, D., Sokolov, B., & Dolgui, A. (2014). The Ripple effect in supply chains: trade-off 'efficiency-flexibility-resilience' in disruption management. *International Journal of Production Research*, 52(7), 2154-2172.
- Ivanov, D., Pavlov, A., Dolgui, A., Pavlov, D. and Sokolov, B., 2016. Disruption-driven supply chain (re)-planning and performance impact assessment with consideration of pro-active and recovery policies. *Transportation Research Part E: Logistics and Transportation Review*, 90, pp.7-24.
- Jabbarzadeh, A., Fahimnia, B., Sheu, J.B. and Moghadam, H.S., 2016. Designing a supply chain resilient to major disruptions and supply/demand interruptions. *Transportation Research Part B: Methodological*, 94, pp.121-149.
- Jaggi, C. K., Tiwari, S., & Goel, S. K. (2017). Credit financing in economic ordering policies for non-instantaneous deteriorating items with price dependent demand and two storage facilities. *Annals of Operations Research*, 248(1-2), 253-280.
- Kamalahmadi, M. and Parast, M.M., 2016. A review of the literature on the principles of enterprise and supply chain resilience: Major findings and directions for future research. *International Journal of Production Economics*, 171, pp.116-133.
- Kamalahmadi, M. and Parast, M.M., 2017. An assessment of supply chain disruption mitigation strategies. *International Journal of Production Economics*, 184, pp.210-230.
- Kaya, O. and Polat, A.L., 2017. Coordinated pricing and inventory decisions for perishable products. *OR spectrum*, 39(2), pp.589-606
- Klibi, W. and Martel, A., 2012a. Modeling approaches for the design of resilient supply networks under disruptions. *International Journal of Production Economics*, 135(2), pp.882-898.
- Klibi, W. and Martel, A., 2012b. Scenario-based supply chain network risk modeling. *European Journal of Operational Research*, 223(3), pp.644-658.
- Klibi, W., Martel, A., Guitouni, A., 2010. The design of robust value-creating supply chain networks: a critical review. *European Journal of Operational Research*. 203 (2), 283–293.
- Klibi, W. and Rice, J.B. and Urciuoli, L. (2018). Special dossier: Quantifying supply chain resilience, *Supply Chain Forum: An International Journal*, 19, 4, 253—254, Taylor & Francis.

- Le Hoa Vo, T., & Thiel, D. (2011). Economic simulation of a poultry supply chain facing a sanitary crisis. *British Food Journal*, 113(8), 1011-1030.
- Liu, M. and Zhang, D., 2016. A dynamic logistics model for medical resources allocation in an epidemic control with demand forecast updating. *Journal of the Operational Research Society*, 67(6), pp.841-852.
- Manning, L., Baines, R. N., & Chadd, S. A. (2005). Deliberate contamination of the food supply chain. *British Food Journal*, 107(4), 225-245.
- Mogale, D.G., Kumar, M., Kumar, S.K. and Tiwari, M.K., 2018. Grain silo location-allocation problem with dwell time for optimization of food grain supply chain network. *Transportation Research Part E: Logistics and Transportation Review*, 111, pp.40-69.
- Mohammed, A. and Wang, Q., 2017a. Multi-criteria optimization for a cost-effective design of an RFID-based meat supply chain. *British Food Journal*, 119(3), pp.676-689.
- Mohammed, A. & Wang, Q., 2017b. The fuzzy multi-objective distribution planner for a green meat supply chain. *International Journal of Production Economics*, 184, pp.47-58.
- Mohammed, A., Wang, Q. and Li, X., 2017. A cost-effective decision-making algorithm for an RFID-enabled HMSC network design: A multi-objective approach. *Industrial Management & Data Systems*, 117(9), pp.1782-1799.
- Mohan, S., Gopalakrishnan, M., Mizzi, P., 2013. Improving the efficiency of a nonprofit supply chain for the food insecure. *International Journal of Production Economics*, 143 (2), 248-255.
- Nooraie, S.V. and Parast, M.M., 2016. Mitigating supply chain disruptions through the assessment of trade-offs among risks, costs and investments in capabilities. *International Journal of Production Economics*, 171, pp.8-21.
- Pearce, R.H. and Forbes, M., 2018. Disaggregated Benders decomposition and branch-and-cut for solving the budget-constrained dynamic un-capacitated facility location and network design problem. *European Journal of Operational Research*, 270(1), pp.78-88.
- Pishvae, M.S., Razmi, J. and Torabi, S.A., 2014. An accelerated Benders decomposition algorithm for sustainable supply chain network design under uncertainty: A case study of medical needle and syringe supply chain. *Transportation Research Part E: Logistics and Transportation Review*, 67, pp.14-38.
- Ponomarov, S., 2012. Antecedents and Consequences of Supply Chain Resilience: a Dynamic Capabilities Perspective. University of Tennessee, Knoxville, Tennessee, United States
- Qi, L., Shen, Z.J.M. and Snyder, L.V., 2010. The effect of supply disruptions on supply chain design decisions. *Transportation Science*, 44(2), pp.274-289.
- Qin, X., Liu, X. and Tang, L., 2013. A two-stage stochastic mixed-integer program for the capacitated logistics fortification planning under accidental disruptions. *Computers & Industrial Engineering*, 65(4), pp.614-623.
- Rong, A., Akkerman, R. and Grunow, M., 2011. An optimization approach for managing fresh food quality throughout the supply chain. *International Journal of Production Economics*, 131(1), pp.421-429.
- Rong, A., & Grunow, M., 2010. A methodology for controlling dispersion in food production and distribution. *Or Spectrum*, 32(4), 957-978.
- San-José, L.A., Sicilia, J. and García-Laguna, J., 2015. Analysis of an EOQ inventory model with partial backordering and non-linear unit holding cost. *Omega*, 54, pp.147-157.
- Santoso, T., Ahmed, S., Goetschalckx, M., Shapiro, A., 2005. A stochastic programming approach for supply chain network design under uncertainty. *European Journal of Operational Research*, 167 (1), pp.96-115.
- Sawik, T., 2013. Selection of resilient supply portfolio under disruption risks. *Omega* 41 (2), 259-269.
- Sawik, T., 2014. Joint supplier selection and scheduling of customer orders under disruption risks: single vs. dual sourcing. *Omega*, 43, pp.83-95.
- Sawik, T., 2018. Disruption Mitigation and Recovery in Supply Chains using Portfolio Approach. *Omega*, 84, pp.232-248.
- Sheffi, Y., 2007. The resilient enterprise: Overcoming vulnerability for competitive advantage. Cambridge, MA: MIT Press.
- Sheffi, Y., 2005. The Resilient Enterprise: Overcoming Vulnerability for Competitive Advantage. MIT Press.

- Shishebori, D. and Babadi, A.Y., 2015. Robust and reliable medical services network design under uncertain environment and system disruptions. *Transportation Research Part E: Logistics and Transportation Review*, 77, pp.268-288.
- Snyder, L.V., Scaparra, M.P., Daskin, M.S. and Church, R.L., 2006. Planning for disruptions in supply chain networks. *Tutorials in operations research*, 2, pp.234-257.
- Soysal, M., Bloemhof-Ruwaard, J.M., Haijema, R. and van der Vorst, J.G., 2015. Modeling an Inventory Routing Problem for perishable products with environmental considerations and demand uncertainty. *International Journal of Production Economics*, 164, pp.118-133.
- Soysal, M., Bloemhof-Ruwaard, J.M. and Van der Vorst, J.G.A.J., 2014. Modelling food logistics networks with emission considerations: The case of an international beef supply chain. *International Journal of Production Economics*, 152, pp.57-70.
- Stone, J. and Rahimifard, S., 2018. Resilience in agri-food supply chains: a critical analysis of the literature and synthesis of a novel framework. *Supply Chain Management: An International Journal*, 23(3), pp.207-238.
- Tang, C.S., 2006. Perspectives in supply chain risk management. *International Journal of production economics*, 103 (2), pp.451-488.
- Tassier, T., 2005. "SIR model of epidemics." *Annual report*.
- Tendall, D.M., Joerin, J., Kopainsky, B., Edwards, P., Shreck, A., Le, Q.B., Krütli, P., Grant, M. and Six, J., 2015. Food system resilience: defining the concept. *Global Food Security*, 6, pp.17-23.
- Terreri, A., 2009. Preventing the next product recall, *Food Logistics* 111- 2025
- Tiwari, S., Jaggi, C. K., Gupta, M., & Cárdenas-Barrón, L. E. (2018). Optimal pricing and lot-sizing policy for supply chain system with deteriorating items under limited storage capacity. *International Journal of Production Economics*, 200, 278-290.
- Torabi, S.A., Namdar, J., Hatefi, S.M. and Jolai, F., 2016. An enhanced possibilistic programming approach for reliable closed-loop supply chain network design. *International Journal of Production Research*, 54(5), pp.1358-1387.
- Tukamuhabwa, B.R., Stevenson, M., Busby, J. and Zorzini, M., 2015. Supply chain resilience: definition, review and theoretical foundations for further study. *International Journal of Production Research*, 53(18), pp.5592-5623.
- Validi, S., Bhattacharya, A. and Byrne, P.J., 2014. A case analysis of a sustainable food supply chain distribution system—A multi-objective approach. *International Journal of Production Economics*, 152, pp.71-87.
- Vlajic, J.V., Van der Vorst, J.G. and Haijema, R., 2012. A framework for designing robust food supply chains. *International Journal of Production Economics*, 137(1), pp.176-189.
- Wagner, S.M. and Neshat, N., 2010. Assessing the vulnerability of supply chains using graph theory. *International Journal of Production Economics*, 126(1), pp.121-129.
- Wang, X. and Li, D., 2012. A dynamic product quality evaluation-based pricing model for perishable food supply chains. *Omega*, 40(6), pp.906-917.
- WHO (2010). Accessible at <https://www.who.int/csr/don/en/>
- Zahiri, B., Jula, P. and Tavakkoli-Moghaddam, R., 2018. Design of a pharmaceutical supply chain network under uncertainty considering perishability and substitutability of products. *Information Sciences*, 423, pp.257-283.
- Zahiri, B., Zhuang, J. and Mohammadi, M., 2017. Toward an integrated sustainable-resilient supply chain: A pharmaceutical case study. *Transportation Research Part E: Logistics and Transportation Review*, 103, pp.109-142.
- Zwietering, M.H., De Wit, J.C. and Notermans, S., 1996. Application of predictive microbiology to estimate the number of *Bacillus cereus* in pasteurised milk at the point of consumption. *International journal of food microbiology*, 30(1-2), pp.55-70.

Appendix A. Monte Carlo procedure and scenario reduction method

In this section, a scenario generation approach is proposed in [Figure A.1](#) based on the epidemic risk modeling and the Monte Carlo sampling. This latter uses pseudo-random numbers and the inverse of the parameters' distribution function of the random variables involved. The outputs of the method are expressed in term ζ_{et}^s , which impact the capacity parameter and also the inventory level in the modeling approach. Running the procedure in [Figure A.1](#) N times yields a sample of independent scenarios $\{s_1, s_2, \dots, s_n, \dots, s_N\}$. In the procedure, u denotes a pseudo-random number, and $F^{-1}(u)$ the inverse of the standardized Normal variate. The proposed Monte Carlo procedure includes five main steps. First, disruption arrival time is generated for each zone based on exponential distribution function. Thus, a chronological list of disruption occurrence is constructed for each zone. Second, for each disruption in the list (γ_z^s), disruption intensity is calculated. After this, a hit test is done for each node in the disrupted zone $z \in Z$. In this step, a chronological list of disruption occurrence is constructed for each node of the network. In the fourth step, propagation of disruption and its time lag in the network is adapted based on distance and relations between nodes, and the contaminated nodes and disruption time periods are obtained. Therefore, in this step, the nodes' chronological disruption list is updated. Fifth, time to recovery is calculated for each disrupted node and the function $g_t(\beta_e^s, \theta_e^s)$ takes binary values (0-1) according to the disrupted time periods, as shown in [Figure 5a](#)). Finally, the disruption impact is calculated as loss parameter ζ_{et}^s . Using the same method, we generate a demand size for each scenario over the planning horizon, where the demand is uniformly distributed.

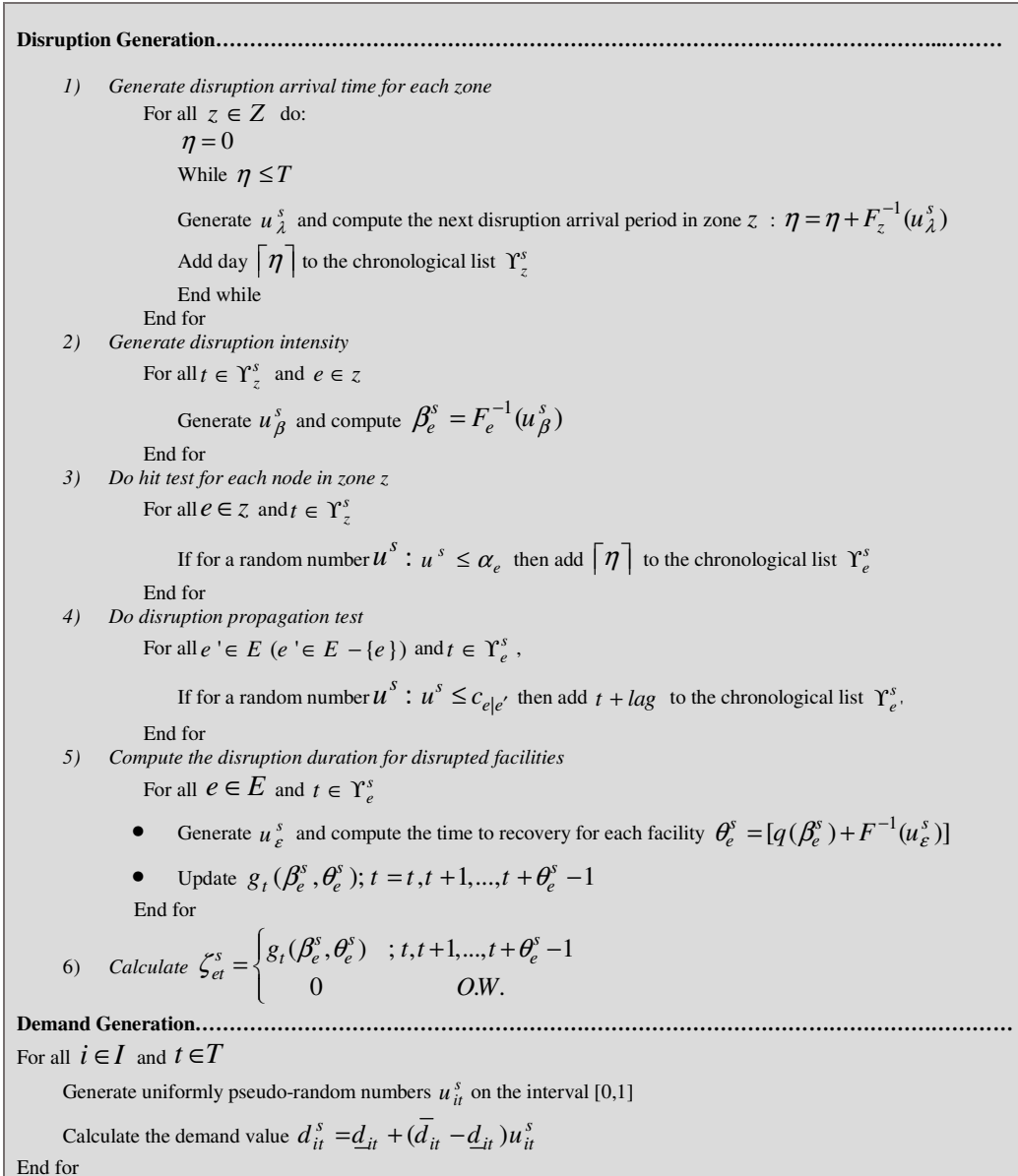


Figure A.1 Monte Carlo Scenario generation procedure for disruption and stochastic demands

The parameters of the Monte Carlo procedure are according to the values indicated in Table 7 as follows.

Table 7 Parameters values of the Monte Carlo procedure

Parameter	u_λ^s	α_e	$c_{e e'}$	θ_e^s
Value	Exprnd(10)	U(0.3,0.4)	U(0.0,0.7)	U(1,4)

It should be noted that according to Figures 5a) and 5b), once the disruption occurs, the capacity and inventory levels drop to zero, so the random parameter u_β^s is equal to 1. Besides, as it was described in Section 3.2, $prop_{e|e'}$ is derived in a correlation matrix based on regional proximity and directional network relations. According to parameters in Table 7, an inter-arrival rate of 20 weeks (10 bi-weekly arrivals) is considered that its conditional hit

probability is 0.4, which correspond jointly to a compound likelihood of epidemic arrival-hit of 1 each 50 weeks per year. This behavior is close to what is observed in practice. It is clear that the avian influenza scenario is an extreme event that not only depends on the arrival rate but on the intensity magnitude, propagation scale and the preparedness level. Besides, these parameters could vary for different kinds of disruptions. For instance, avian influenza could diffuse smoothly but COVID-19 would show a considerable outbreak leading to a pandemic.

Fuzzy Bezdek Clustering Method

Next, let us introduce the basics of the FCM method, employed here to cluster the scenarios. We consider a set of S scenarios $X = \{x_1, x_2, \dots, x_S\}$ in a R^p dimensional space, and FCM method tries to partition these scenarios into C ($1 < C < S$) fuzzy clusters. According to our epidemic risk modeling approach (Figure A.1), we have considered two attributes (P) for each scenario, namely number of hits and total disrupted capacity of the SC. The FCM (adopted from Bezdek, 1974) consists of five iterative steps, as follows. The output of the method is to provide a reduced subset of scenarios, where each scenario is among the existing ones and is representative of a given cluster.

Step 1 Fix the desired number of clusters C , the weighing exponent m , the induced A-norm on R^n and $r=0$. Generate an initial membership matrix (U_0). The membership matrix determines membership degrees of scenarios to each cluster.

$$U = \begin{bmatrix} u_{11} & \dots & u_{1S} \\ \dots & u_{cs} & \dots \\ u_{C1} & \dots & u_{CS} \end{bmatrix} ; 0 \leq u_{cs} \leq 1 \ \& \ \sum_{c=1}^C u_{cs} = 1 \quad (\text{A.1})$$

where u_{cs} is the membership degree of the s^{th} scenario to the c^{th} cluster center.

Step 2 Compute the cluster center vector CC. Where γ_s is the main characteristic of scenario s .

$$CC = \left[\left(\sum_{s=1}^S u_{1s}^m \cdot \gamma_s / \sum_{s=1}^S u_{1s} \right) \dots \left(\sum_{s=1}^S u_{Cs}^m \cdot \gamma_s / \sum_{s=1}^S u_{Cs} \right) \right]^{-1} ; 1 \leq m < \infty \quad (\text{A.2})$$

Step 3 Calculate the new membership matrix (U^{r+1}) according to Equations (A.3) and (A.4)

$$u_{cs}^{r+1} = \left[\sum_{j=1}^C \left(\frac{u_{cs}^r}{u_{js}^r} \right)^{\frac{2}{m-1}} \right]^{-1} \quad (\text{A.3})$$

$$U^{r+1} = \begin{bmatrix} u_{11}^{r+1} & \dots & u_{1S}^{r+1} \\ \dots & u_{cs}^{r+1} & \dots \\ u_{C1}^{r+1} & \dots & u_{CS}^{r+1} \end{bmatrix} \quad (\text{A.4})$$

Step 4 If $U^{r+1} - U^r < \varepsilon$ (tolerance level) stop; otherwise set $r = r + 1$ and return to step 2

Step 5 Attribute $\pi_c = \sum_{s=1}^S u_{cs} \pi_s$ to each cluster center as the likelihood of occurrence of that cluster center.

Appendix B. Benders Decomposition Formulation

Primal Sub-Problem (PSP)

$$Z1 = \text{Max} \sum_{i \in I} \sum_{r \in T} \sum_{t \in T} \sum_{s \in S} \omega_{irt} y_{irt}^s -$$

$$\left(\begin{aligned} & \sum_{p \in P} \sum_{n \in N} f_{pn} \overline{L_{pn}} + \sum_{d \in D} \sum_{k \in K} f_{dk} \overline{L_{dk}} + \sum_{p \in P} \sum_{t \in T} \sum_{s \in S} c_p Pr_{pt}^s + \sum_{p \in P} \sum_{d \in D} \sum_{t \in T} \sum_{r \in T} \sum_{s \in S} c_{pd} x_{pdr}^s + \sum_{d \in D} \sum_{i \in I} \sum_{t \in T} \sum_{r \in T} \sum_{s \in S} c_{di} x_{dir}^s \\ & + \sum_{p \in P} \sum_{r \in T} \sum_{t \in T} \sum_{s \in S} h_{prt} \left(\frac{I_{prt-1}^s + I_{prt}^s}{2} \right) + \sum_{d \in D} \sum_{r \in T} \sum_{t \in T} \sum_{s \in S} h_{drt} \left(\frac{I_{drt-1}^s + I_{drt}^s}{2} \right) + \sum_{i \in I} \sum_{r \in T} \sum_{t \in T} \sum_{s \in S} h_{irt} \left(\frac{I_{irt-1}^s + I_{irt}^s}{2} \right) \\ & + \sum_{p \in P} \sum_{t \in T} \sum_{s \in S} ce_{pt} E_{pt}^s + \sum_{d \in D} \sum_{t \in T} \sum_{s \in S} ce_{dt} E_{dt}^s + \sum_{i \in I} \sum_{t \in T} \sum_{s \in S} ce_{it} E_{it}^s + \sum_{i \in I} \sum_{t \in T} \sum_{s \in S} ls_{it} D_{it}^{-s} \end{aligned} \right)$$

B.1

$$x_{dir}^s \leq M \overline{A_{id}} \quad dv_{dirts}^6 \quad \forall d \in D, i \in I, r \& t \in T, s \in S \mid 0 \leq t - r \leq SL \quad \text{B.2}$$

$$x_{pdr}^s \leq M \sum_n \overline{L_{pn}} \quad dv_{pdrts}^7 \quad \forall p \in P, d \in D, r \& t \in T, s \in S \mid 0 \leq t - r \leq SL \quad \text{B.3}$$

$$Pr_{pt}^s - I_{prt}^s - \sum_{d \in D} x_{pdr}^s = 0 \quad dv_{prts}^8 \quad \forall p \in P, r \& t \in T \mid r = t, s \in S \quad \text{B.4}$$

$$I_{prt}^s - I_{pr(t-1)}^s + \sum_{d \in D} x_{pdr}^s = 0 \quad dv_{prts}^9 \quad \forall p \in P, r \& t \in T \mid 0 < t - r \leq SL, s \in S \quad \text{B.5}$$

$$\sum_{r \in T} I_{prt}^s - E_{pt}^s = 0 \quad dv_{pts}^{10} \quad \forall p \in P, t \in T \mid t - r = SL, s \in S \quad \text{B.6}$$

$$\sum_{p \in P} x_{pdr}^s - I_{drt}^s - \sum_{i \in I} x_{dir}^s = 0 \quad dv_{drts}^{11} \quad \forall d \in D, r \& t \in T \mid r = t, s \in S \quad \text{B.7}$$

$$I_{drt}^s - I_{dr(t-1)}^s - \sum_{p \in P} x_{pdr}^s + \sum_{i \in I} x_{dir}^s = 0 \quad dv_{drts}^{12} \quad \forall d \in D, r \& t \in T \mid 0 < t - r \leq SL, s \in S \quad \text{B.8}$$

$$\sum_{r \in T} I_{drt}^s - E_{dt}^s = 0 \quad dv_{dts}^{13} \quad \forall d \in D, t \in T, s \in S \quad \text{B.9}$$

$$\sum_{d \in D} x_{dir}^s - I_{irt}^s - y_{irt}^s = 0 \quad dv_{ints}^{14} \quad \forall i \in I, r \& t \in T \mid r = t, s \in S \quad \text{B.10}$$

$$I_{irt}^s - I_{ir(t-1)}^s - \sum_{d \in D} x_{dir}^s + y_{irt}^s = 0 \quad dv_{ints}^{15} \quad \forall i \in I, r \& t \in T \mid 0 < t - r \leq SL, s \in S \quad \text{B.11}$$

$$\sum_{r \in T} I_{irt}^s - E_{it}^s = 0 \quad dv_{its}^{16} \quad \forall i \in I, t \in T, s \in S \quad \text{B.12}$$

$$-\sum_{r \in T} y_{irt}^s \leq -d_{it} \quad dv_{its}^{17} \quad \forall i \in I, t \in T \mid 0 \leq t - r \leq SL, s \in S \quad \text{B.13}$$

$$\sum_{r \in T} y_{irt}^s + D_{it}^- = d_{it}^s \quad dv_{its}^{18} \quad \forall i \in I, t \in T \mid 0 \leq t - r \leq SL, s \in S \quad \text{B.14}$$

$$Pr_{pr}^s \leq q_{pr} \quad dv_{prs}^{19} \quad \forall p \in P, r \in T, s \in S \quad \text{B.15}$$

$$\sum_{d \in D} \sum_{r \in T} x_{pdr}^s \leq \sum_n cap_{pn} \overline{L_{pn}} \quad dv_{pts}^{20} \quad \forall p \in P, t \in T, s \in S \quad \text{B.16}$$

$$\sum_{i \in I} \sum_{r \in T | 0 \leq t - r \leq SL} x_{dir}^s \leq \sum_k cap_{dk} \overline{L_{dk}} \quad dv_{dts}^{21} \quad \forall d \in D, t \in T, s \in S \quad \text{B.17}$$

$$\sum_{r \in T | 0 \leq t - r \leq SL} I_{irt}^s \leq cap_i \quad dv_{its}^{22} \quad \forall i \in I, t \in T, s \in S \quad \text{B.18}$$

$$L_{pn}, L_{dk}, A_{id} \in \{0, 1\} \quad \forall i \in I, n \in N, d \in D, m \in M, p \in P \quad \text{B.19}$$

$$x_{pdn}^s, x_{din}^s, Pr_{pt}^s, I_{prt}^s, I_{drt}^s, I_{irt}^s, Ex_{it}^s, y_{irt}^s \geq 0 \quad \forall p \in P, d \in D, i \in I, r \in T, t \in T, s \in S \quad \text{B.20}$$

Dual Sub-Problem (DSP)

$$\begin{aligned} \text{Minimizing} \quad & \sum_{\substack{d, i, r, t, s \\ 0 \leq t - r \leq SL}} dv_{dirts}^6 (-M \times \overline{A_{id}}) + \sum_{\substack{p, d, r, t, s \\ 0 \leq t - r \leq SL}} dv_{pdrts}^7 (-M \sum_n \overline{L_{pn}}) + \sum_{i, t, s} dv_{its}^{17} (\underline{d}_{it}) + \sum_{i, t, s} dv_{its}^{18} (d_{it}^s) + \\ & \sum_{p, r, s} dv_{prs}^{19} (-q_p) + \sum_{p, t, s} dv_{pts}^{20} (-\sum_n cap_{pn} \overline{L_{pn}}) + \sum_{d, t, s} dv_{dts}^{21} (-\sum_k cap_{dk} \overline{L_{dk}}) + \sum_{i, t, s} dv_{its}^{22} (-cap_i) \end{aligned} \quad \text{B.21}$$

$$-dv_{dirts}^6 - dv_{dirts}^{11} + dv_{irts}^{14} - dv_{dts}^{21} \geq -c_{di} \quad \forall d \in D, i \in I, r \text{ \& } t \in T \mid t = r, s \in S \quad \text{B.22}$$

$$-dv_{dirts}^6 + dv_{dirts}^{12} - dv_{irts}^{15} - dv_{dts}^{21} \geq -c_{di} \quad \forall d \in D, i \in I, r \text{ \& } t \in T \mid r < t, s \in S \quad \text{B.23}$$

$$-dv_{pdrts}^7 - dv_{prts}^9 + dv_{dirts}^{11} - dv_{pts}^{20} \geq -c_{pd} \quad \forall p \in P, d \in D, r \text{ \& } t \in T \mid t = r, s \in S \quad \text{B.24}$$

$$-dv_{pdrts}^7 + dv_{prts}^9 - dv_{dirts}^{12} - dv_{pts}^{20} \geq -c_{pd} \quad \forall p \in P, d \in D, r \text{ \& } t \in T \mid r < t, s \in S \quad \text{B.25}$$

$$-d_{prts}^8 - dv_{pr(t+1)s}^9 \geq -\frac{1}{2}(h_{prn} + h_{pr(t+1)}) \quad \forall p \in P, r \text{ \& } t \in T \mid t = r, s \in S \quad \text{B.26}$$

$$+dv_{prts}^9 - dv_{pr(t+1)s}^9 \geq -\frac{1}{2}(h_{prn} + h_{pr(t+1)}) \quad \forall p \in P, r \text{ \& } t \in T \mid t > r \text{ \& } t - r \leq SL, s \in S \quad \text{B.27}$$

$$+dv_{prts}^9 - dv_{pr(t+1)s}^9 + dv_{pts}^{10} \geq -\frac{1}{2}(h_{prn} + h_{pr(t+1)}) \quad \forall p \in P, r \text{ \& } t \in T \mid t - r = SL, s \in S \quad \text{B.28}$$

$$-dv_{dirts}^{11} - dv_{dr(t+1)s}^{12} \geq -\frac{1}{2}(h_{drn} + h_{dr(t+1)}) \quad \forall d \in D, r \text{ \& } t \in T \mid t = r, s \in S \quad \text{B.29}$$

$$+dv_{dirts}^{12} - dv_{dr(t+1)s}^{12} \geq -\frac{1}{2}(h_{drn} + h_{dr(t+1)}) \quad \forall d \in D, r \text{ \& } t \in T \mid t > r \text{ \& } t - r \leq SL, s \in S \quad \text{B.30}$$

$$+dv_{dirts}^{12} - dv_{dr(t+1)s}^{12} + dv_{dts}^{13} \geq -\frac{1}{2}(h_{drn} + h_{dr(t+1)}) \quad \forall d \in D, r \text{ \& } t \in T \mid t - r = SL, s \in S \quad \text{B.31}$$

$$-dv_{irts}^{14} - dv_{ir(t+1)s}^{15} - dv_{its}^{22} \geq -\frac{1}{2}(h_{irn} + h_{ir(t+1)}) \quad \forall i \in I, r \text{ \& } t \in T \mid t = r, s \in S \quad \text{B.32}$$

$$+dv_{irts}^{15} - dv_{ir(t+1)s}^{15} - dv_{its}^{22} \geq -\frac{1}{2}(h_{irn} + h_{ir(t+1)}) \quad \forall i \in I, r \text{ \& } t \in T \mid t > r \text{ \& } t - r \leq SL, s \in S \quad \text{B.33}$$

$$+dv_{irts}^{15} - dv_{ir(t+1)s}^{15} - dv_{its}^{22} + dv_{its}^{16} \geq -\frac{1}{2}(h_{irn} + h_{ir(t+1)}) \quad \forall i \in I, r \text{ \& } t \in T \mid t - r = SL, s \in S \quad \text{B.34}$$

$$\sum_{t \in T} d_{prts}^8 - dv_{prts}^{19} \geq -c_p \quad \forall p \in P, r \in T \mid t = r, s \in S \quad \text{B.35}$$

$$dv_{its}^{18} \geq -ls_{it} \quad \forall i \in I, t \in T, s \in S \quad \text{B.36}$$

$$-dv_{irts}^{14} + dv_{its}^{17} + dv_{its}^{18} \geq \omega_{it} \quad \forall i \in I, r \text{ \& } t \in T \mid t = r, s \in S \quad \text{B.37}$$

$$dv_{irts}^{15} + dv_{its}^{17} + dv_{its}^{18} \geq \omega_{it} \quad \forall i \in I, r \text{ \& } t \in T \mid t > r \text{ \& } t - r \leq SL, s \in S \quad \text{B.38}$$

$$dv_{pts}^{10} \geq -ce_{pt} \quad \forall p \in P, t \in T, s \in S \quad \text{B.39}$$

$$dv_{dts}^{13} \geq -ce_{dt} \quad \forall d \in D, t \in T, s \in S \quad \text{B.40}$$

$$dv_{its}^{16} \geq -ce_{it} \quad \forall i \in I, t \in T, s \in S \quad \text{B.41}$$

Master Problem (MP)

$$Z = Max \left(-\sum_{p \in P} \sum_{n \in N} f_{pn} L_{pn} - \sum_{d \in D} \sum_{k \in K} f_{dk} L_{dk} \right) \quad \text{B.42}$$

$$\sum_n L_{pn} \leq 1 \quad \forall p \in P \quad \text{B.43}$$

$$\sum_k L_{dk} \leq 1 \quad \forall d \in D \quad \text{B.44}$$

$$A_{id} \leq \sum_k L_{dk} \quad \forall i \in I, d \in D \quad \text{B.45}$$

$$\sum_{d \in D} A_{id} = 1 \quad \forall i \in I \quad \text{B.46}$$

$$L_{pn}, L_{dk}, A_{id} \in \{0,1\} \quad \forall i \in I, d \in D, p \in P, n \in N, k \in K \quad \text{B.47}$$

Optimality and Feasibility Cuts

$$lb \geq \sum_{p \in P} \sum_{n \in N} f_{pn} L_{pn} + \sum_{d \in D} \sum_{k \in K} f_{dk} L_{dk} + \sum_{\substack{d,i,r,t,s \\ 0 \leq t-r \leq SL}} \overline{dv_{dirts}^{7iter}} [-M \times A_{id}] + \sum_{\substack{p,d,r,t,s \\ 0 \leq t-r \leq SL}} \overline{dv_{pdrts}^{8iter}} [-M \sum_n L_{pn}] + \sum_{i,t,s} \overline{dv_{its}^{15iter}} [d_{it}] + \sum_{i,t,s} \overline{dv_{its}^{16iter}} [d_{it}^s] + \text{B.48}$$

$$\sum_{p,r,s} \overline{dv_{prs}^{17iter}} [-q_p] + \sum_{p,t,s} \overline{dv_{pts}^{18iter}} [-\sum_n cap_{pn} L_{pn}] + \sum_{d,t,s} \overline{dv_{dts}^{19iter}} [-\sum_k cap_{dk} L_{dk}] + \sum_{i,t,s} \overline{dv_{its}^{20iter}} [-cap_i] \quad \text{B.49}$$

$$0 \geq \sum_{\substack{d,i,r,t,s \\ 0 \leq t-r \leq SL}} \overline{dv_{dirts}^{7iter}} [-M \times A_{id}] + \sum_{\substack{p,d,r,t,s \\ 0 \leq t-r \leq SL}} \overline{dv_{pdrts}^{8iter}} [-M \sum_n L_{pn}] + \sum_{i,t,s} \overline{dv_{its}^{15iter}} [d_{it}] + \sum_{i,t,s} \overline{dv_{its}^{16iter}} [d_{it}^s] + \sum_{p,r,s} \overline{dv_{prs}^{17iter}} [-q_p] + \sum_{p,t,s} \overline{dv_{pts}^{18iter}} [-\sum_n cap_{pn} L_{pn}] + \sum_{d,t,s} \overline{dv_{dts}^{19iter}} [-\sum_k cap_{dk} L_{dk}] + \sum_{i,t,s} \overline{dv_{its}^{20iter}} [-cap_i]$$